

Air Force Institute of Technology

**AFIT Scholar**

---

Theses and Dissertations

Student Graduate Works

---

3-5-2007

## Direct Diode Pumped Raman Amplifier Based on a Multimode Graded Index Fiberr

Charles James Baird

Follow this and additional works at: <https://scholar.afit.edu/etd>



Part of the [Optics Commons](#)

---

### Recommended Citation

Baird, Charles James, "Direct Diode Pumped Raman Amplifier Based on a Multimode Graded Index Fiberr" (2007). *Theses and Dissertations*. 2908.

<https://scholar.afit.edu/etd/2908>

This Thesis is brought to you for free and open access by the Student Graduate Works at AFIT Scholar. It has been accepted for inclusion in Theses and Dissertations by an authorized administrator of AFIT Scholar. For more information, please contact [richard.mansfield@afit.edu](mailto:richard.mansfield@afit.edu).



**DIRECT DIODE PUMPED RAMAN AMPLIFIER BASED ON A  
MULTIMODE GRADED INDEX FIBER**

THESIS

C. James Baird, Captain, USAF

AFIT/GAP/ENP/07-01

**DEPARTMENT OF THE AIR FORCE  
AIR UNIVERSITY**

***AIR FORCE INSTITUTE OF TECHNOLOGY***

**Wright-Patterson Air Force Base, Ohio**

APPROVED FOR PUBLIC RELEASE; DISTRIBUTION UNLIMITED

The views expressed in this thesis are those of the author and do not reflect the official policy or position of the United States Air Force, Department of Defense, or the United States Government.

AFIT/GAP/ENP/07-01

DIRECT DIODE PUMPED RAMAN AMPLIFIER BASED ON  
A MULTIMODE GRADED INDEX FIBER

THESIS

Presented to the Faculty  
Department of Engineering Physics  
Graduate School of Engineering and Management  
Air Force Institute of Technology  
Air University  
Air Education and Training Command  
In Partial Fulfillment of the Requirements for the  
Degree of Master of Science (Applied Physics)

C. James Baird  
Captain, USAF

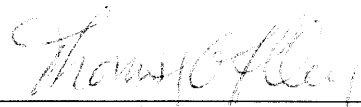
March 2007

APPROVED FOR PUBLIC RELEASE; DISTRIBUTION UNLIMITED

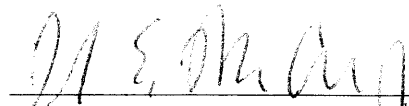
DIRECT DIODE PUMPED RAMAN AMPLIFIER BASED ON A  
MULTIMODE GRADED INDEX FIBER

C. James Baird  
Captain, USAF

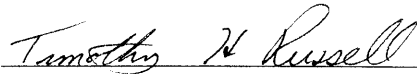
Approved:

  
\_\_\_\_\_  
Thomas G. Alley (Chairman)

5 Mar 2007  
Date

  
\_\_\_\_\_  
Jack E. McCrae (Member)

5 Mar 2007  
Date

  
\_\_\_\_\_  
Timothy H. Russell (Member)

5 MAR 2007  
Date

*Abstract*

The direct pumping of a Raman fiber amplifier (RFA) was attempted using an array of four 25W, fiber pigtailed diodes at 936nm, combined via a 7 channel fiber beam combiner. The initial attempt was conducted using a 1.8 km, 100  $\mu\text{m}$  core, GRIN fiber with an NA of .29 and attenuation 3.6 dB/km at 936nm. While amplification was not achieved, over 200mW of conversion was shown, with 10.4W of pump power and 3.5W of seed. This corresponds to an average conversion efficiency of 2.2%. The subsequent effort utilized a 2km long, 200  $\mu\text{m}$  core, GRIN fiber, with NA of .27 and attenuation of 2.8dB/km at pump wavelength. Again, amplification was not achieved, but a gain of 80mW was present, with 3.5W of seed power and 14W of pump. This corresponds to an average conversion efficiency of 0.6% and only 2.5% of the coupled seed power. The final experiment attempted to solve the problem of coupling efficiency and high Raman threshold by utilizing a 50/250 dual-clad fiber, with NAs of .28 and .46 for the core and inner cladding, respectively. Again, amplification was not realized, as only 100mW of gain was present, with 25W of pump and 4.2W of coupled seed power, corresponding to 36% of the coupled seed, and an average conversion efficiency of only 0.4%. Although amplification was not achieved for any of the three fibers, gain was shown possible in all, showing that directly pumping an RFA with a diode source is possible.

## *Acknowledgements*

I would first like to extend my utmost appreciation to my advisor, Lt Col Tom Alley, for his guidance and knowledge throughout the past 18 months. Without his constant encouragement and insight, I have no doubt my efforts would not have come to fruition. Also, I would like to extend my thanks to Maj Timothy Russell, who was there when my advisor couldn't be, and helped me understand many of the theories and physics behind my experiment. Thanks also go out to my fellow students, Capt Nate Terry, who helped me find my way around the lab, and Maj Massey and Lt Gamboa, who were there with suggestions when I ran into so many problems. Most of all, thanks to my lovely soon-to-be wife for the patience and understanding when I was at school until midnight. You're what kept me going through all the hard times.

C. James Baird

## *Table of Contents*

	Page
Abstract . . . . .	iv
Acknowledgements . . . . .	v
List of Figures . . . . .	viii
List of Abbreviations . . . . .	xi
<b>I. Introduction . . . . .</b>	<b>1-1</b>
1.1 <b>Background . . . . .</b>	1-1
1.2 <b>Motivation . . . . .</b>	1-2
1.3 <b>Experiment Objectives and Limitations . . . . .</b>	1-3
<b>II. Literature Review . . . . .</b>	<b>2-1</b>
2.1 <b>Chapter Overview . . . . .</b>	2-1
2.2 <b>Fiber Optics . . . . .</b>	2-1
2.3 <b>Numerical Aperture . . . . .</b>	2-2
2.4 <b>Etendue . . . . .</b>	2-3
2.5 <b>Attenuation . . . . .</b>	2-4
2.6 <b>Fiber Coupling . . . . .</b>	2-4
2.7 <b>Beam Quality . . . . .</b>	2-5
2.8 <b>Introduction to Nonlinear Optics . . . . .</b>	2-6
2.9 <b>Stimulated Raman Scattering . . . . .</b>	2-7
2.10 <b>Raman Gain and Threshold . . . . .</b>	2-8
2.11 <b>Raman Fiber Amplifiers . . . . .</b>	2-11
2.12 <b>Relevant Research . . . . .</b>	2-13
2.13 <b>Summary . . . . .</b>	2-14
<b>III. Single Diode Pumped 100 <math>\mu\text{m}</math> GRIN 1.8 km RFA . . . . .</b>	<b>3-1</b>
3.1 <b>Experimental Setup . . . . .</b>	3-1
3.2 <b>Diagnostic Equipment Description . . . . .</b>	3-3
3.3 <b>Experiment 1 Results . . . . .</b>	3-3
3.3.1 <b>Spectrum Data . . . . .</b>	3-3
3.3.2 <b>Power Data . . . . .</b>	3-4
3.4 <b>Summary . . . . .</b>	3-7



	Page
IV. <b>Multi Diode Pumped 100 <math>\mu\text{m}</math> GRIN 1.8 km RFA</b> . . . . .	4-1
4.1 <b>Experimental Setup</b> . . . . .	4-1
4.2 <b>Experiment 2 Results</b> . . . . .	4-2
4.2.1 <b>Spectrum Data</b> . . . . .	4-2
4.2.2 <b>Power Data</b> . . . . .	4-4
4.3 <b>Beam Quality</b> . . . . .	4-6
4.4 <b>Summary</b> . . . . .	4-7
V. <b>Multi Diode Pumped 200 <math>\mu\text{m}</math> core GRIN 2 km RFA</b> . . . . .	5-1
5.1 <b>Experimental Setup</b> . . . . .	5-1
5.2 <b>Experiment 3 Results</b> . . . . .	5-1
5.2.1 <b>Spectrum Data</b> . . . . .	5-1
5.2.2 <b>Power Data</b> . . . . .	5-3
5.3 <b>Beam Quality</b> . . . . .	5-4
5.4 <b>Summary</b> . . . . .	5-4
VI. <b>Multi Diode Pumped 50/250 DCF 500m RFA</b> . . . . .	6-1
6.1 <b>Experimental Setup</b> . . . . .	6-1
6.2 <b>Experiment 4 Results</b> . . . . .	6-2
6.2.1 <b>Spectrum Data</b> . . . . .	6-2
6.2.2 <b>Power Data</b> . . . . .	6-4
6.3 <b>Beam Quality</b> . . . . .	6-6
6.4 <b>Summary</b> . . . . .	6-6
VII. <b>Conclusions and Recommendations</b> . . . . .	7-1
7.1 <b>Results of this work</b> . . . . .	7-1
7.2 <b>Suggestions for Future Work</b> . . . . .	7-2
Appendix A. <b>Calculating Raman Threshold</b> . . . . .	A-1
Bibliography . . . . .	BIB-1

## List of Figures

Figure		Page
2.1.	Index of refraction profile for both a step index core fiber (left) and graded index (GRIN) fiber (right). . . . .	2-2
2.2.	Diagram of a dual-clad fiber. The core, typically single mode, is surrounded by the lower index inner cladding, which is responsible for guiding the light into the core. The outer cladding confines the light to the inner cladding, and is of lower index still. The buffer adds mechanical strength to the fiber, and is usually stripped away during the coupling process. . . . .	2-3
2.3.	Energy diagram for both the Stokes and Anti-Stokes shifts. In the Stokes shift, an incoming photon will excite the ground state electron to a higher virtual state, with the electron then relaxing to a lower state and emitting a photon corresponding to that shift. Anti-Stokes shift occurs when the incoming photon excites an already excited electron, which then relaxes to the ground state and emits a photon of higher energy. $V_f$ and $V_i$ are the final and initial energy levels of the electron. . . . .	2-8
2.4.	Raman-gain spectrum of fused silica. Figure from <i>Encyclopedia of Laser Physics and Technology (10)</i> . . . . .	2-9
2.5.	Schematic diagrams of both a backward seeded RFA (top), and forward seeded configuration (bottom) . . . . .	2-12
3.1.	The attenuation curve, as reported by the manufacturer, of the NuFern 100 $\mu\text{m}$ diameter core, GRIN fiber. . . . .	3-1
3.2.	Experiment #1 setup. Pump laser is a fiber pigtailed, LIMO diode laser at 938nm, while the seed laser is also a LIMO, but at 978nm. 20x objective lenses were used to both collimate and focus the pump beam and seed beam into the gain fiber. D1 and D2 are diagnostic points. . . . .	3-2
3.3.	Spectrum results of both the forward (red) and backward (blue) directions for the single diode pumped, unseeded RFA based on the 1.8 km NuFern GRIN 100 $\mu\text{m}$ core fiber. The unseeded spectrum verifies there is no Stokes conversion of the pump, even at maximum pump power. . . . .	3-4
3.4.	Spectrum data for the .5 W seeded configuration based on the 1.8 km NuFern GRIN 100 $\mu\text{m}$ core fiber. The spectrum shows the spectrum of the backward Stokes in blue and the residual pump in red. The slight shift in the pump wavelength peak between the two points can be attributed to a lack of warm-up time for the pump laser. . . . .	3-5
3.5.	Spectrum for the 1.3 W seeded single diode pumped RFA configuration based on the 1.8 km NuFern GRIN 100 $\mu\text{m}$ core fiber. . . . .	3-5
3.6.	Single diode pumped residual pump power data for the unseeded, .5 W seeded, and 1.3 W seeded configurations. . . . .	3-6
3.7.	Single diode pumped backward Stokes power data for the unseeded, .5 W seeded, and 1.3 W seeded configurations. . . . .	3-6

Figure	Page	
4.1.	Schematic of experiment 2. All 4 pump diodes are collimated using 20x microscope objectives, and subsequently focus into the squid with 16x objectives. Again, D1 and D2 are diagnostic points. . . . .	4-2
4.2.	Spectrum for the unseeded multi-diode pumped RFA configuration based on the 1.8 km NuFern GRIN 100 $\mu\text{m}$ core fiber. . . . .	4-3
4.3.	Spectrum for the 3.5 W seeded multi-diode pumped RFA configuration based on the 1.8 km NuFern GRIN 100 $\mu\text{m}$ core fiber. . . . .	4-3
4.4.	Multi-diode pumped residual pump power data for the unseeded and 3.5 W seeded configurations for the 100 $\mu\text{m}$ core GRIN fiber. . . . .	4-4
4.5.	Multi-diode pumped backward Stokes power data for the unseeded and 3.5 W seeded configurations based on the 100 $\mu\text{m}$ core GRIN fiber. . . . .	4-5
4.6.	The Stokes conversion efficiency for Experiment 2. The average for this experiment is approximately 2.2%, with the peak being 6.25%. . . . .	4-5
4.7.	Measurement errors for the multi-diode pumped RFA based on the 100 $\mu\text{m}$ core, 1.8 km long GRIN fiber. Error includes power fluctuations in the laser and calibration of power meters. . . . .	4-6
4.8.	Schematic of the camera placement for taking $M^2$ measurements. . . . .	4-7
5.1.	Schematic of experiment 3. Identical to that of experiment 2, but with a 2km NuFern 200 $\mu\text{m}$ core GRIN fiber as the gain medium. D1 and D2 are diagnostic points. Again, a 16x microscope objective was determined to be the most efficient at coupling the pump power into the gain fiber. . . . .	5-2
5.2.	Spectrum for the unseeded multi-diode pumped RFA configuration based on the 2 km NuFern GRIN 200 $\mu\text{m}$ core fiber. . . . .	5-2
5.3.	Spectrum for the 3.5 W seeded multi-diode pumped RFA configuration based on the 2 km NuFern GRIN 200 $\mu\text{m}$ core fiber. . . . .	5-3
5.4.	Multi-diode pumped residual pump power data for the unseeded and 3.5 W seeded configurations based on the 200 $\mu\text{m}$ core GRIN fiber. A decrease in the maximum residual pump power of approximately 800mW between the unseeded and seeded configuration is shown. . . . .	5-4
5.5.	Multi-diode pumped backward Stokes power data for the unseeded and 3.5 W seeded configurations based on the 200 $\mu\text{m}$ core GRIN fiber. Based on spectrum results, no Stokes was generated in the unseeded experiment, but over 650mW is shown with a seed present, at maximum pump power of 14 watts. . . . .	5-5
5.6.	The Stokes conversion efficiency for Experiment 3. The average for this experiment is approximately 0.6%, with the peak being 1.3%. . . . .	5-5
5.7.	Measurement errors for the multi-diode pumped RFA based on the 200 $\mu\text{m}$ core, 2 km long GRIN fiber. Error includes power fluctuations in the laser and calibration of power meters. . . . .	5-6
6.1.	Schematic of experiment 4. Again, all 4 pump diodes are combined using the squid, with 36 watts of total output. The gain fiber used is a 50/250 NuFern GRIN core fiber at 500m in length. D1 and D2 are diagnostic points. The spatial filter for the seed was left in place to enhance the beam quality being coupled into the fiber. . . . .	6-2

Figure	Page
6.2. Spectrum for the unseeded multi-diode pumped RFA configuration based on the 500m NuFern GRIN 50/250 $\mu\text{m}$ DCF fiber. . . . .	6-3
6.3. Spectrum for the 4.2 W seeded multi-diode pumped RFA configuration based on the 500m NuFern GRIN 50/250 $\mu\text{m}$ DCF fiber. . . . .	6-3
6.4. Multi-diode pumped residual pump power data for the unseeded and 4.2 W seeded configurations based on the 50/250 $\mu\text{m}$ core DCF GRIN fiber. A decrease in the maximum residual pump power of approximately 800mW between the unseeded and seeded configuration is shown. . . . .	6-4
6.5. Multi-diode pumped backward Stokes power data for the unseeded and 4.2 W seeded configurations based on the 50/250 $\mu\text{m}$ core DCF GRIN fiber. Based on spectrum results, no Stokes was generated in the unseeded experiment, but over 1.5 watts is shown with a seed present, at maximum pump power of 25.1 watts. . . . .	6-5
6.6. The Stokes conversion efficiency for Experiment 4. The average for this experiment is approximately 0.4%, with the peak being 0.8%. . . . .	6-5
6.7. Measurement errors for the multi-diode pumped RFA based on the 50/250 $\mu\text{m}$ core, .5 km long GRIN DCF fiber. Error includes power fluctuations in the laser and calibration of power meters. . . . .	6-6

*List of Abbreviations*

Abbreviation		Page
ABL	Airborne Laser . . . . .	1-1
THEL	Tactical High Energy Laser . . . . .	1-1
COIL	Chemical Oxygen Iodine Laser . . . . .	1-1
DOD	Department of Defense . . . . .	1-1
RFL	Raman Fiber Laser . . . . .	1-2
SRS	Stimulated Raman scattering . . . . .	1-2
RFA	Raman fiber amplifier . . . . .	1-2
GRIN	Graded index . . . . .	2-1
DCF	Dual clad fiber . . . . .	2-2
NA	Numerical aperture . . . . .	2-2
BPP	Beam parameter product . . . . .	2-5
SBS	Stimulated Bragg Scattering . . . . .	2-7
FWM	Four wave mixing . . . . .	2-11

# DIRECT DIODE PUMPED RAMAN AMPLIFIER BASED ON A MULTIMODE GRADED INDEX FIBER

## I. Introduction

### 1.1 *Background*

With the future now upon us, the use of lasers as a practical weapon is now becoming reality, thanks to the Air Force's Airborne Laser (ABL) and the Army's Tactical High Energy Laser (THEL) programs. These laser systems utilize a high power, chemical laser to focus sustained energy onto a target, thereby destroying it. While both system have been proven effective in tests, neither has seen any real combat situations. This is due largely to the complicated logistics support these types of lasers require. Most chemical lasers require large cooling systems, making them bulky and very difficult to mobilize, as the ABL has shown. The main laser for the ABL is a multi-hundred kilowatt chemical oxygen iodine laser (COIL) developed in the 1970's by the Air Force Weapons Lab Phillips Lab (6), which fires an infrared beam. The COIL laser requires four different chemicals to operate: hydrogen peroxide, potassium hydroxide, chlorine gas, and Iodine, which are constantly pumped through the system. The logistical footprint needed to constantly supply these chemicals is significant. But what if the military were able to use a lighter, high power laser that requires only air cooling, is electrically powered, and is available in a large number of wavelengths? This is why the Department of Defense (DOD) has shown growing interest in fiber lasers in the past few years.

Fiber lasers have shown a boost in popularity in both commercial and industrial applications, due in large part to their good beam quality and potentially high power outputs. They are typically pumped by electrically powered, semiconductor lasers, which require only minimal cooling, but can also be pumped using a variety of other types of lasers, depending on the application. While power limits for fiber lasers and

amplifiers are only in the kilowatt range, the ability to combine multiple fiber lasers provides the potential for much greater outputs, challenging that of lasers like the COIL. And because fiber lasers need only to be air-cooled, their mobility is much greater than other laser systems with equivalent power, making them very appealing the future DOD projects.

## ***1.2 Motivation***

A specific type of fiber laser, Raman fiber lasers (RFL) were initially confined to the telecommunications industry, which required the good beam quality these types of lasers provide. Because of this, early RFLs were limited to the use of single mode fibers as the gain medium. This severely limited the amount of power that could be produced, but allowed for the necessary high beam quality, as higher modes were not allowed to propagate in the fiber. To get greater power out, one must create an RFL that uses a larger core area, multimode fiber as the gain medium. Doing this will greatly increase the amount of power that can be coupled in, but consequently limit the beam quality. Multimode fiber-based RFLs with near single mode output have been shown possible in the past (2), but scaling the output power to higher levels has been a problem. Because the larger core fiber can push the threshold power needed to achieve the Stimulated Raman Scattering (SRS) effect, necessary for the operation of RFLs, to near impossible limits for a single mode pump source, a Raman Fiber Amplifier (RFA) can be used instead. RFAs work on the same SRS principle of RFLs, which will be discussed in more detail below, but introduces a seed beam that propagates at the output wavelength of the system, thereby lowering the pump power needed to achieve SRS. This seed beam can propagate in the same direction as the pump beam (forward seeded), or in opposite directions (backward seeded), each direction having respective benefits and drawbacks. As is the case with RFLs, RFAs are typically pumped with a high beam quality, single mode fiber pump source.

### *1.3 Experiment Objectives and Limitations*

Typical Raman Fiber Amplifiers are pumped using a high beam quality, single mode fiber laser, thereby creating an inefficient chain of lasers, as the fiber laser used for pumping needs to be pumped as well. The purpose of this experiment is to remove the fiber laser from the chain, and pump the RFA directly, with a series of fiber-pigtailed, semiconductor diode lasers. The RFA will be based on a 1.8 km long, multimode fiber, which is a good match for the output fiber of the diodes, but also places the lower bound on the Raman threshold at approximately 65W, assuming only single mode operation, which makes a seed laser necessary. The method used to calculate this threshold power will be shown in greater detail later. By removing the intermediate fiber laser from the chain, and using a multimode fiber as the gain medium, the overall efficiency and power of the system should be much higher, as should the output power of the amplifier. To make this possible, several issues need to be addressed. First, the coupling efficiency between the diode fibers and the gain fiber will need to be optimized. Because free space coupling will be used to combine the fibers, the optimal microscope objective combination will need to be determined to allow for maximum coupling of the pump light. Next, will the use of a fiber beam combiner allow for significant pump power needed to reach the Raman threshold? Because the output fiber of the fiber beam combiner is larger than the gain fiber, insufficient coupling efficiency between the two may limit the amount of pump power allowed into the gain fiber. Finally, the poor beam quality of both the pump and seed lasers may not allow for enough mode overlap to achieve pump-to-Stokes conversion. Because of this, these sources may also need to be spatially filtered, which will greatly limit the power allowed into the fiber.



## II. Literature Review

### 2.1 Chapter Overview

The purpose of this chapter is to familiarize the reader with the physics and techniques applicable to this research topic. First, the physics of fiber optics is introduced, followed by an introduction to nonlinear optics. Subsequently the concepts of Stimulated Raman Scattering and Raman threshold are discussed. A short introduction to Raman fiber amplifiers is presented next, followed finally by a brief examination of significant research related to this subject matter.

### 2.2 Fiber Optics

An optical fiber is a dielectric waveguide based on the principle of total internal reflection (TIR). This is made possible due to the difference in the indices of refraction of the cross-section, propagating along the length of the fiber. The index of refraction,  $n$ , is a ratio describing how fast light travels in a certain material, and is found by (7)

$$n = c/v_p. \quad (2.1)$$

where  $c$  is the speed of light in a vacuum and  $v_p$  is the phase velocity of light in the material. In a majority of standard fibers, a cladding whose index is slightly lower surrounds a central core with a high index of refraction. In a graded index fiber (GRIN), like the one used in this experiment, the core of the fiber has an index profile that decreases with radial distance from the center. The profile for many GRIN fibers can often be approximated using a parabolic curve. The advantage in using a GRIN fiber over a traditional, step index fiber is decreased modal dispersion, or differences in the group velocities of the spatial modes. This property is best exploited for use in long distance communications, for which it was developed. A typical, large mode area fiber, be it step or graded index core, will allow for more power, but poorer beam quality. A GRIN core, however, can produce a high quality Stokes beam, through the process of Stimulated Raman Scattering, which will be discussed in greater detail below. It is because of this property that the experiments for this research are focused

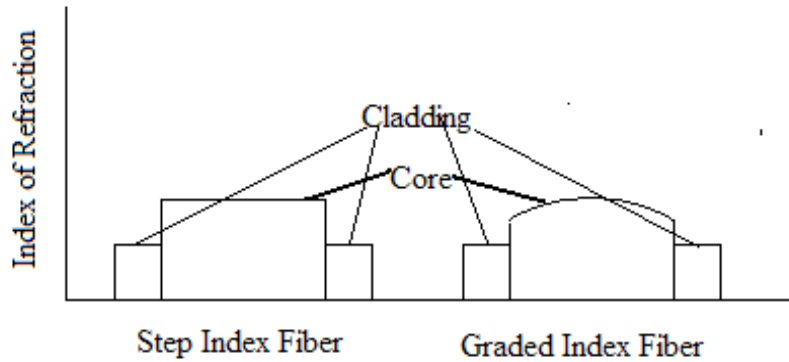


Figure 2.1: Index of refraction profile for both a step index core fiber (left) and graded index (GRIN) fiber (right).

on graded index core fibers. Index profiles for both step and graded index fibers can be seen below.

Another type of fiber commonly used in fiber lasers is the dual clad fiber, or DCF. The core of a DCF is surrounded by two layers of respectively lower index cladding. The inner cladding is responsible for guiding light in the core, while the outer layer confines the light in the inner cladding. The core of DCFs are most commonly single mode, which only guides light with good beam quality. A poor quality beam, like the diode pump source used in this experiment, can propagate in both the core and inner cladding, depending on the mode, while the generated Stokes beam may be confined to just the core.

### 2.3 Numerical Aperture

One of the most important parameters to understand when working with fiber optics is the numerical aperture, or NA. The NA of a fiber is a measure of the maximum acceptance angle that can be coupled into the core, and is dependent on the refractive index difference between the core and the cladding. For a step index fiber, the NA is determined by

$$NA = n \sin \theta_{\max} = \sqrt{n_f^2 - n_c^2}. \quad (2.2)$$

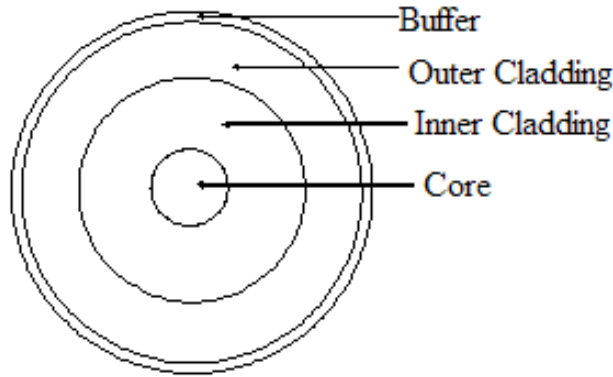


Figure 2.2: Diagram of a dual-clad fiber. The core, typically single mode, is surrounded by the lower index inner cladding, which is responsible for guiding the light into the core. The outer cladding confines the light to the inner cladding, and is of lower index still. The buffer adds mechanical strength to the fiber, and is usually stripped away during the coupling process.

where  $\theta_{\max}$  is the maximum half angle of acceptance,  $n_f$  is the index of refraction of the fiber core, and  $n_c$  is the index of the cladding. This factor is most important when dealing with the coupling of light between fibers, as differences in the  $NA$  of two fibers can significantly reduce the overall coupling efficiency and result in fiber facet damage at higher powers. Manufacturers rate their fibers based on core size, index profile,  $NA$ , and wavelength attenuation.

## 2.4 Etendue

When coupling two fibers of different sizes together, an important value to know is the etendue of each fiber. Etendue is a measure of how well the beam leaving the fiber can be focused, and the ratio of these will determine the maximum amount of light that can be coupled between the two, due to the conservation of etendue principle. This value is calculated a number of ways, including the area of the source times the solid angle subtended from the entrance pupil, or the area of the entrance pupil times the solid angle subtended from the source. However, the best method to use when comparing two fibers is the mode area of the fiber times it's solid angle of

acceptance. The ratio of the etendues reduces to a simpler form, and can simply be expressed as the fiber's NA times is core area, or:

$$\frac{NA_i^2 d_i^2}{NA_e^2 d_e^2} = C_{eff\ max} \quad (2.3)$$

Where  $NA_i^2 d_i^2$  is the numerical aperture times the square of the core diameter of the incident fiber, and  $NA_e^2 d_e^2$  is the same for the exiting fiber. This value will provide the maximum coupling efficiency percentage between two fibers,  $C_{eff\ max}$ .

## 2.5 Attenuation

The attenuation of a fiber is a wavelength dependent measurement of all losses that occur within the fiber. It is conventional to express this value in terms of dB/km, which is related to loss per length by (1)

$$\alpha_{dB} = -\left(\frac{10}{L}\right) \text{Log}_{10}\left(\frac{P_T}{P_0}\right) = 4.343\alpha_p. \quad (2.4)$$

where  $P_T$  is transmitted power through the fiber,  $P_0$  is coupled power, and  $L$  is fiber length. Knowing the fiber's attenuation and length, one can calculate the fiber's effective length,  $L_{eff}$ , which is the length of a corresponding, non-attenuated fiber that possesses an equivalent gain volume. This value is very helpful in calculating other parameters in fiber optics, including Raman gain and threshold, which are covered below.

$$L_{eff} = \frac{[1 - \exp(-\alpha_p L)]}{\alpha_p}. \quad (2.5)$$

## 2.6 Fiber Coupling

There are only a limited number of ways to join two fibers together efficiently, among them are fusion splicing, butt connecting, and free-space coupling. Fusion splicing (8) is the most efficient way to achieve a good connection, as it essentially welds the two fibers together to form a seamless and low-loss joint. The downfall of this method is that it can require a rather expensive machine and a great deal of

time to obtain the correct “recipe” for an ideal connection. The second type of splice is the butt-connection, which can be accomplished by placing the two ends of the fiber face-to-face, and placing a clamp on both ends to secure them in place, or by fitting the fiber ends with connectors, and screwing them together. Although more efficient than free-space coupling, this method poses a higher risk of fiber damage if not correctly aligned. The last approach, free-space coupling, is the method used in this experiment. Free-space coupling uses a series of lenses to first collimate the beam leaving one fiber, and then focus the beam into the other. While it is considered the most inefficient means of coupling, it does allow for fibers of different sizes and NAs to be coupled more readily.

## 2.7 Beam Quality

One final value to make note of is beam quality. While it is closely associated with lasers, beam quality is important to fiber optics as well, and the nature of this experiment warrants a brief explanation of the measurement. The most accepted value of beam quality in fibers today is  $M^2$ , or the beam quality factor.  $M^2$  compares the profile of the beam in question to that of a true Gaussian beam, and is based on the ratios of the beam parameter product (BPP) of both. The BPP is the product of the beam radius at the beam waist, and it’s maximum divergence half-angle. True Gaussian beams will have the lowest BPP possible,  $\lambda/\pi$ , where  $\lambda$  is the the wavelength of beam. Therefore, the lowest  $M^2$  value a beam can have is 1, which is typically assumed for single mode fibers. This factor will limit how small a beam can be focused, for a specific divergence angle, and is determined by

$$w(z) = w_0 \sqrt{1 + \left( \frac{M^2 \lambda (z - z_0)}{\pi w_0^2} \right)^2}. \quad (2.6)$$

where  $w_0$  is the radius of the beam at the waist,  $\lambda$  is the wavelength of the beam,  $w(z)$  is the radius of the beam at  $z$ , and  $z_0$  is the distance to the beam waist.

## 2.8 Introduction to Nonlinear Optics

Maxwell's equations govern the behavior of electromagnetic waves in matter. In differential form they are

$$\nabla \cdot \vec{D} = \rho. \quad (2.7)$$

$$\nabla \cdot \vec{B} = 0. \quad (2.8)$$

$$\nabla \times \vec{E} = -\frac{\partial \vec{B}}{\partial t}. \quad (2.9)$$

$$\nabla \times \vec{H} = \vec{J} + \frac{\partial \vec{D}}{\partial t}. \quad (2.10)$$

where  $\vec{E}$  is the electric field,  $\vec{D}$  is the electric displacement field,  $\vec{B}$  is the magnetic induction,  $\vec{H}$  is the magnetic field,  $\vec{J}$  is the free current density, and  $\rho$  is the free charge density. When there is no free charge present, then equation 2.7 becomes

$$\nabla \cdot \vec{D} = 0. \quad (2.11)$$

The electric displacement field is then related to the electric field  $\vec{E}$ , and polarization  $\vec{P}$  by (7)

$$\vec{D} = \epsilon \vec{E} = \epsilon_0 \vec{E} + \vec{P}. \quad (2.12)$$

The field of nonlinear optics studies the behavior of light in a material where a strong electric field is applied, resulting in an induced, nonlinear polarization. The polarization,  $\vec{P}$ , is defined by

$$\vec{P}_i = \epsilon_0 \chi_{ij}^{(1)} \vec{E}_j + \epsilon_0 \chi_{ijk}^{(2)} \vec{E}^2 + \epsilon_0 \chi_{ijkl}^{(3)} \vec{E}^3 \dots \quad (2.13)$$

where  $\epsilon_0$  is the electric permittivity the material and  $\chi^n$  is the  $n^{\text{th}}$  order electric susceptibility tensor. The first order  $\chi$  describes the linear effects of materials, including index of refraction and absorption characteristics. The second order  $\chi$  is associated with nonlinear effects in material, such as second harmonic generation, parametric mixing and amplifying, and the Pockels effect. Third order non-linear effects, gov-

erned by the third order susceptibility tensor, are where many optical phenomenon take place, including Stimulated Broullion Scattering (SBS) and Stimulated Raman Scattering (SRS). Many materials possess these higher-order optical properties, but their contribution to the material's overall polarization is insignificant in the absence of a strong electric field, and is very often ignored.

## 2.9 *Stimulated Raman Scattering*

First observed in 1928 by C.V. Raman, the Raman effect is described as the downshifting of a photon's frequency as a result of interaction with molecules in a medium. When the wavelength of the incoming photon is downshifted, the resultant radiation is referred to as the Stokes photon, and when the frequency is upshifted, the photon is called the anti-Stokes. The frequency of the Stokes and anti-Stokes photon can be respectively determined by

$$\omega_s = \omega_p - \Omega_{fg}. \quad (2.14)$$

$$\omega_{as} = \omega_p + \Omega_{fg}. \quad (2.15)$$

where  $\Omega_{fg}$  is the materials vibration frequency and  $\omega_p$  is the frequency if the incoming photon. A quantum-mechanical diagram of both the Stokes and anti-Stokes generation can be seen below. In the case of the Stokes photon, an incoming photon is annihilated and causes a molecule in the ground state to excite to a higher-energy virtual state. This molecule then relaxes to a lower state, but not before giving off a photon of frequency  $\omega_s$ , or the Stokes photon. In the case of the anti-Stokes photon, the incoming photon is again annihilated, but causes a molecule in an already excited state to transition to a higher virtual state. The molecule then decays all the way to the ground state, and gives off a photon of higher energy, with frequency  $\omega_{as}$ , or the anti-Stokes photon.

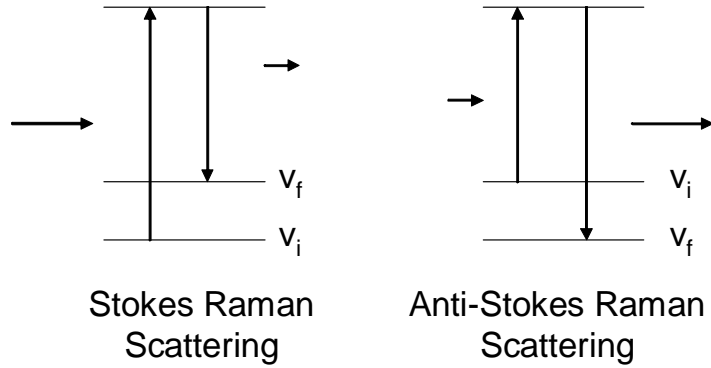


Figure 2.3: Energy diagram for both the Stokes and Anti-Stokes shifts. In the Stokes shift, an incoming photon will excite the ground state electron to a higher virtual state, with the electron then relaxing to a lower state and emitting a photon corresponding to that shift. Anti-Stokes shift occurs when the incoming photon excites an already excited electron, which then relaxes to the ground state and emits a photon of higher energy.  $V_f$  and  $V_i$  are the final and initial energy levels of the electron.

### 2.10 Raman Gain and Threshold

In 1962, it was observed that high pump powers can yield a rapid growth of Stokes photons in a medium, creating an stimulated Raman effect in which much of the pump energy is transferred to the Stokes output (12). The Stokes wave is a result of a large number of Stokes photons, and the growth of this wave is governed by (1)

$$\frac{dI_s}{dz} = g_R I_p I_s - \alpha_s I_s. \quad (2.16)$$

$$\frac{dI_p}{dz} = - \left( \frac{\omega_p}{\omega_s} \right) g_R I_p I_s - \alpha_p I_p. \quad (2.17)$$

where  $I_p$  is the pump intensity,  $I_s$  is the Stokes intensity,  $g_R$  is the Raman gain coefficient, and  $\alpha_s$  and  $\alpha_p$  are losses in the fiber at the Stokes and pump frequencies respectively. Dependent on the composition of the material,  $g_R$  varies heavily with  $\Omega$ , or the frequency difference between the pump and Stokes frequencies. For pure silica, based on a frequency shift of 13.2 THz,  $g_R$  is approximately  $1 * 10^{-13} m/W$ . This pa-



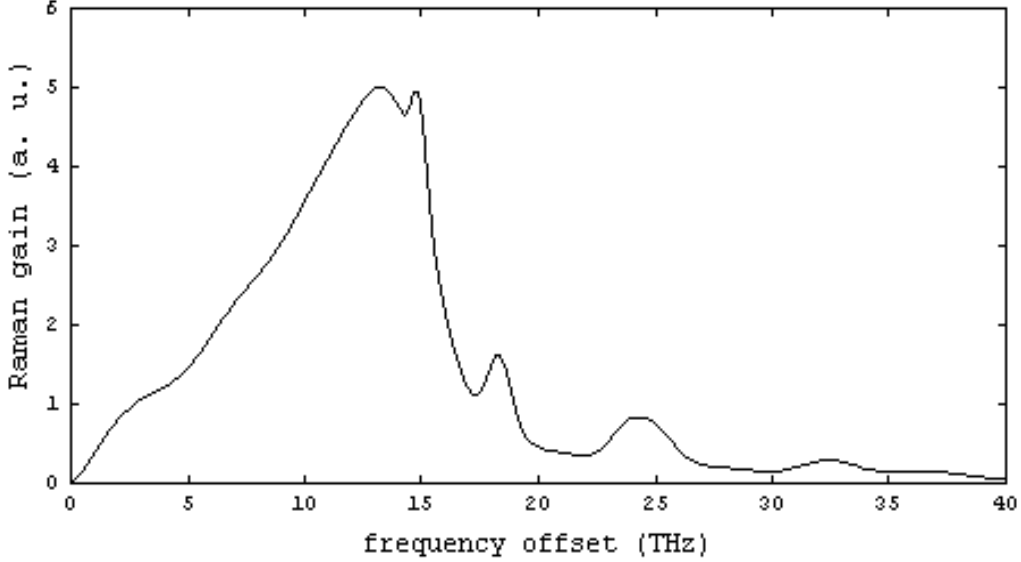


Figure 2.4: Raman-gain spectrum of fused silica. Figure from *Encyclopedia of Laser Physics and Technology* (10).

parameter gives rise to the Raman-gain spectrum, which is the most important quantity in describing SRS. The frequency of the subsequent Stokes wave is determined by the peak of the Raman gain for that particular material and pump frequency. In many crystalline materials, Raman scattering is limited to specific, well-defined bands. But in amorphous solids, such as silica, the vibrational frequencies are allowed to spread out over a large range, creating an ideal gain spectrum for achieving threshold, as shown in figure 2.4.

As shown in Agrawal (1), to calculate the Stokes power one must first integrate over the entire range of the Raman-gain spectrum. Carrying out this integration gives

$$P_s(L) = P^{eff} \exp[g_R(\Omega_R)I_0L_{eff} - \alpha_s L]. \quad (2.18)$$

where

$$P^{eff} = \hbar\omega_s B_{eff}. \quad (2.19)$$

and the effective bandwidth is

$$B_{eff} = \left( \frac{2\pi}{I_0 L_{eff}} \right)^{1/2} \left| \frac{\partial^2 g_R}{\partial \omega^2} \right|_{\omega=\omega_s}^{-1/2}. \quad (2.20)$$

The Raman threshold condition, defined as the input pump power at which the generated Stokes power and output pump power are equal, is given by

$$P^{eff} \exp\left(\frac{g_R P_0 L_{eff}}{A_{eff}}\right) = P_0. \quad (2.21)$$

With  $P_0$  equal to the input pump power, the solution to this equation, for a single pass condition, is given by equation 2.22, assuming a Lorentzian line shape for the Raman-gain spectrum and a forward generated Stokes wave. It also assumes that the polarization of both the Stokes and pump is maintained throughout the fiber. If this is not the case, and the polarization is random, then the threshold is increased by a factor of 2. In the case of a Raman fiber amplifier, as the one focused on in this research, the Stokes is created in a backward direction relative to the pump, and the 16 can be replaced with 20 in eq. 2.22.

$$P_{th} = \frac{16A_{eff}}{g_R L_{eff}}. \quad (2.22)$$

The  $A_{eff}$ , or effective core area for a Gaussian approximated single mode can be approximated by

$$A_{eff} = \pi w^2. \quad (2.23)$$

In equation 2.23,  $w$  is the mode width parameter, which, for a graded index fiber is

$$w = a \left( \sqrt{\frac{2}{V}} + \frac{0.23}{V^{3/2}} + \frac{18.01}{V^6} \right). \quad (2.24)$$

and the  $V$  parameter is determined by

$$V = 2\pi \frac{a}{\lambda_0} NA. \quad (2.25)$$

where  $a$  is the radius of the fiber core,  $\lambda_0$  is the propagating wavelength, and  $NA$  is the numerical aperture of the fiber at that particular wavelength. By assuming single mode propagation in the fiber, one is able to place a lower bound on the pump power necessary to achieve the Raman threshold. The calculation of this value for the  $100\ \mu\text{m}$  core GRIN fiber used in this experiment was 65W, and can be seen in Appendix A. To place an upper bound on the threshold power, one must assume that the modes can propagate throughout the entire cross-sectional area of the fiber, not just the effective area. Doing so yields a value of 3150W for the fiber mentioned above, and the calculation can again be seen in Appendix A.

### ***2.11 Raman Fiber Amplifiers***

First developed in 1976 for the fiber-optic communications industry, Raman fiber amplifiers use the Raman effect to amplify a weak “seed” signal. The seed signal is typically of higher wavelength than the pump, and must lie near the peak of the Raman-gain spectrum. These configurations can have either a forward or backward pumped geometry, both of which have been experimentally proven to experience approximately the same gain when polarizations are matched and maintained. See figure 2.5. However, it has been shown by J.Morgan (9) that pumping in the backward geometry greatly reduces the problem of four-wave mixing (FWM), in which the FWM causes the Stokes wave to automatically cascade to higher order Stokes wavelengths, limiting the power of the first order shift. An example of both forward and backward seeded configurations are shown in figure 2.5.

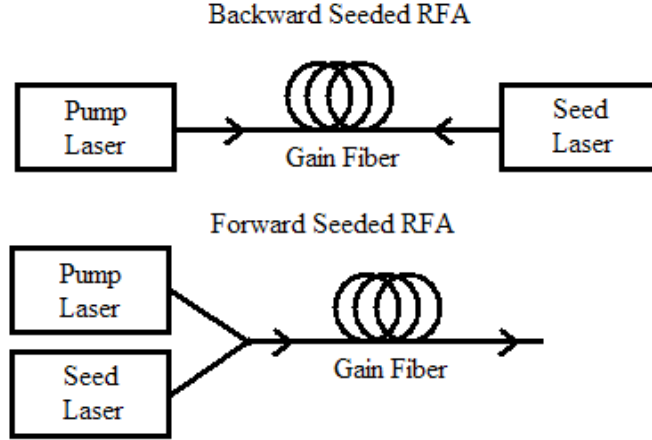


Figure 2.5: Schematic diagrams of both a backward seeded RFA (top), and forward seeded configuration (bottom)

The performance of RFAs is characterized by their amplification factors. The unsaturated amplification factor for an RFA is given by (1)

$$G_A = \exp \left[ \frac{g_R P_0 L_{eff}}{A_{eff}} \right]. \quad (2.26)$$

and the saturated factor is

$$G_s = \frac{1 + r_0}{r_0 + G_A^{-(1+r_0)}}. \quad (2.27)$$

where  $r_0$  is

$$r_0 = \frac{\omega_p P_s(0)}{\omega_s P_0}. \quad (2.28)$$

where  $P_s(0)$  is the output signal power.

One of the greatest advantages of RFAs are the high powers available at wavelengths not achievable from conventional lasers. The reason for this is the many different types of lasers that can be used as pumps. While not used to pump traditional single mode fiber-based RFAs, the use of diode lasers as pump sources allows for a great deal a flexibility, as the output Stokes wavelength is dependent on the pump wavelength, and the large number of different diode wavelengths available makes it

very attractive for a variety of different applications. In order to achieve these high powered, good quality output beams, a high power pump laser with good beam quality is needed, which is one of the main drawbacks to this type of system. This is typically achieved by using a high power, single mode fiber laser as the pump source, which creates a chain of different laser systems, as the fiber laser needs to be pumped as well. The focus of this research is to replace this inefficient chain of pump lasers with an array of smaller, medium power diodes via a squid-like fiber beam combiner. These diodes are fiber pigtailed with multimode fibers, and will be used to directly pump a multimode gain fiber, instead of the single mode gain fiber used in most RFAs.

### ***2.12 Relevant Research***

The main focus of this experiment is to show that it is possible to achieve gain in a Raman fiber using poor beam quality diodes to pump the RFA. Based on previous research, documented below, not only should gain be realized, but beam quality should be improved as well.

One of the inherent properties of SRS is that the generated Stokes beam favors lower order mode propagation, resulting in better beam quality than the pump. In a 1992 paper by Chiang (2), it was shown that, although the  $50\ \mu\text{m}$  core fiber used was multimode, the lower order mode Stokes allowed the fiber to imitate a single mode fiber with regard to the generated beam. Chiang then hypothesized that even with a larger core, multimode fiber, which would allow for more coupled pump power, the generated Stokes beam would still propagate at low order modes. In 2004, Baek and Roh were able to take a pump beam, with an  $M^2$  of 7.0, and produce a Stokes beam with  $M^2$  of only 1.66 in a multimode Raman fiber laser setup, while in 2006, Flusche (4) was able to produce a beam of  $M^2=1.5$  from a pump of  $M^2=42$ , further reinforcing Chiang's hypothesis. It is important to note that these experiments were all unseeded configurations. When the Stokes beam is seeded, as is the practice in RFAs, beam cleanup properties are still evident, and can be improved upon, given a high quality

seed beam. In a paper by Terry et al. (5), both forward and backward seeded setups are explored, in a multimode fiber, for these beam cleanup properties. The results indicate an  $M^2$  of 2.6 and 2.0 for the amplified seed beam, in the backward and forward geometries respectively, from a launched seed  $M^2$  of 2.6 and 3.7, showing no apparent cleanup in the backward direction. In this experiment, an unseeded Stokes beam was created, with  $M^2$  of 1.4, but once a multimode seed was introduced, the output beam quality was limited by the input seed beam quality, for both directions. This proves that beam cleanup does still occur in a seeded, multimode fiber based setup, but is dependent on the quality of the input seed, and also the direction in which the amplifier is seeded.

### ***2.13 Summary***

This chapter introduced the physics of fiber optics to the reader, including the properties of numerical aperture, attenuation, and beam quality. Nonlinear optics was subsequently introduced, with Stimulated Raman Scattering, Raman gain and threshold, and Raman fiber amplifiers being the focal point of this section. Finally, relevant research was presented, including work in SRS beam cleanup and low mode order Stokes generation.

### III. Single Diode Pumped 100 $\mu\text{m}$ GRIN 1.8 km RFA

#### 3.1 Experimental Setup

Before combining the multiple diode pumps via the fiber beam combiner, it was necessary to demonstrate the possibility of gain within the fiber of interest. For this initial experiment, a 1.8 km length of NuFern fiber, with a graded index core size of 100  $\mu\text{m}$  and NA of .29 was used. Based on the manufacturer's data, which can be seen below, the attenuation constant at the pump wavelength, 938nm, was reported to be 3.6 dB/km, and 2.8dB/km at the Stokes wavelength.

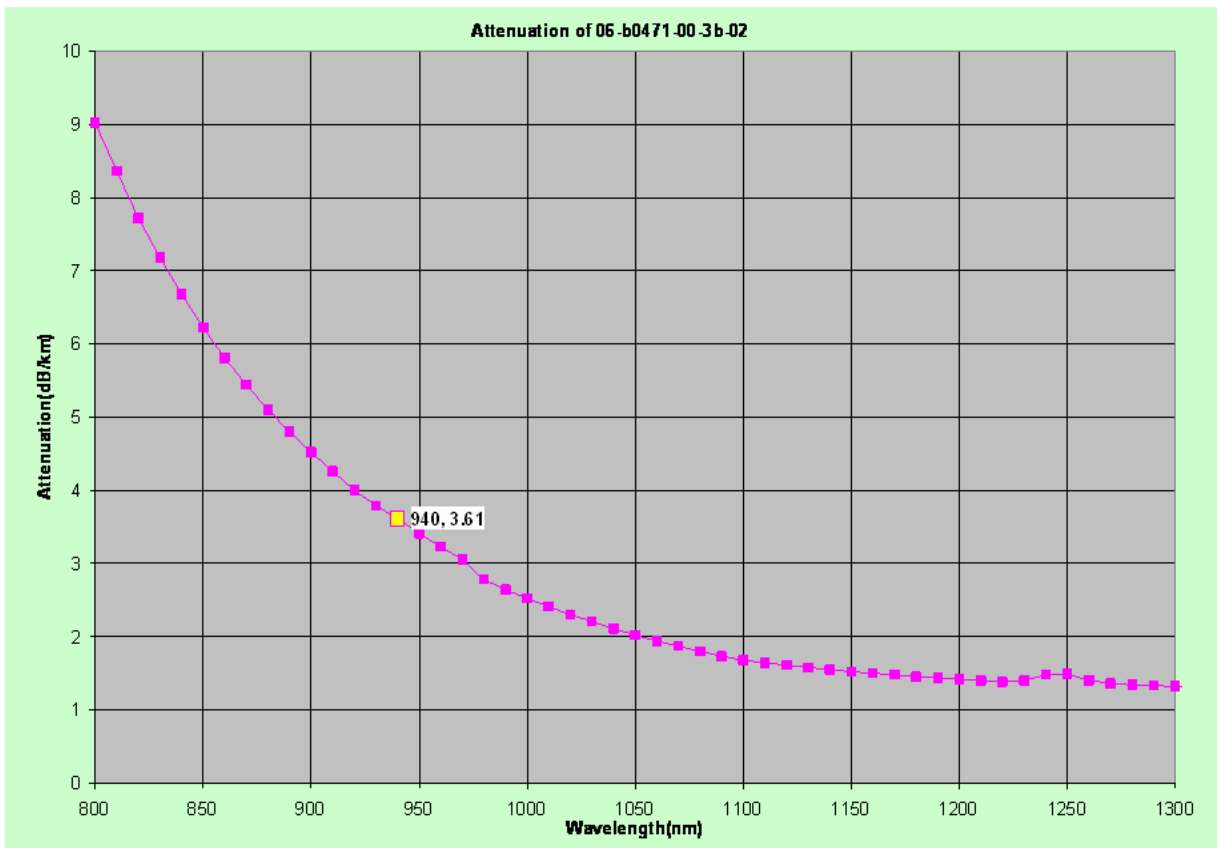


Figure 3.1: The attenuation curve, as reported by the manufacturer, of the NuFern 100  $\mu\text{m}$  diameter core, GRIN fiber.

Based on the known pump wavelength, the Raman shift, of approximately 440  $\text{cm}^{-1}$ , was estimated to produce a Stokes wavelength of 978 nm. A LIMO brand, fiber pigtailed diode laser was used for both pump and seed lasers. The following is a schematic of the backward seeded Raman fiber amplifier experimental setup

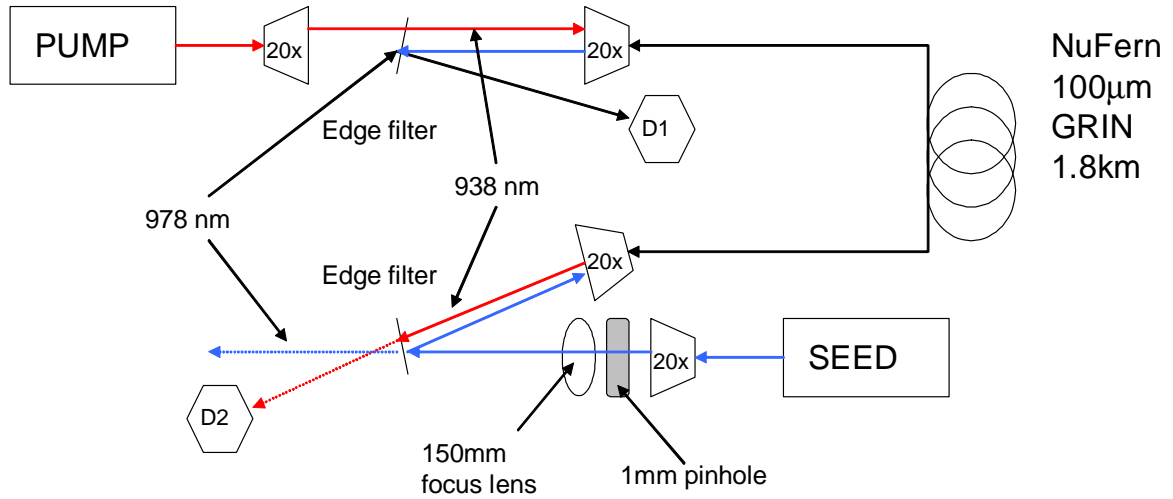


Figure 3.2: Experiment #1 setup. Pump laser is a fiber pigtailed, LIMO diode laser at 938nm, while the seed laser is also a LIMO, but at 978nm. 20x objective lenses were used to both collimate and focus the pump beam and seed beam into the gain fiber. D1 and D2 are diagnostic points.

While both pump and seed are LIMO brand lasers, the pump laser is pigtailed with a 100  $\mu\text{m}$  core fiber of .22 NA, and the seed is pigtailed with a 200  $\mu\text{m}$ , .22 NA fiber. Because the seed laser has a larger diameter output fiber, it was necessary to refocus the beam with the 150mm focus lens to achieve a much higher coupling efficiency into the gain fiber. The 1mm pinhole was used as a spatial filter in hopes that the seed beam quality would also be improved. In addition, the spatial filter allowed for much higher incident seed power without the risk of burning the fiber, as most of the beam that was not focused into the core during free-space coupling was incident on the cladding. To separate the pump and seed beams, edge filters were used at both ends of the fiber. Both filters are rated at less than 95% transmissive for the pump wavelength, and less than 90% reflective for the Stokes, both at normal incidence.



### ***3.2 Diagnostic Equipment Description***

All power measurements were taken with either a Newport brand model 1815-C power meter with a 818-SA head, for powers  $<2$  watts, or a ThorLabs brand 30 watt power meter for  $>2$  watts. Both instruments were calibrated to within  $\pm .5$  mW of each other. All beam quality factor measurements were taken using the Coherent brand Labmaster model, Modemaster camera. This tool allows for much easier and accurate  $M^2$  measurements, giving both X and Y directions  $M^2$  simultaneously, as well as a weighted average of the two.  $M^2$  measurements were taken for the pump, seed, and amplified seed beams. Spectrum measurements were taken of residual pump and generated backward Stokes beams for all unamplified and amplified configurations, at maximum pump and seed powers, using a Ando AQ 6315-B Optical Spectrum Analyzer.

### ***3.3 Experiment 1 Results***

***3.3.1 Spectrum Data.*** For this experiment, 3 different configurations were tested: unseeded, .5 watts of seed, and 1.3 watts of seed. Spectrum data for the unseeded configuration, seen in figure 3.3, shows no backward Stokes generation, so all power measurements taken are of residual pump power in both directions. The reader should note that the scale of spectrum measurements is based on a relative scale set by the optical spectrum analyzer, and not a direct relation of power between the two measurements. Both forward and backward direction spectrum readings were placed on the same plot so the findings could be easily compared. Data for the .5 watts of seed power can be seen in figure 3.4, and shows both pump and backward Stokes spectrums as well. No Stokes generation is evident in the forward direction, but a sharp Stokes peak in the backward output is noticeable. Note the shift in the lasing wavelength of the pump for forward versus backward direction. This is most likely due to temperature and current fluctuations in the diode laser, as a result of insufficient time given for the pump laser to stabilize. The spectrum for the 1.3 W seeded scenario is seen in figure 3.5. Again, the results show no Stokes generation

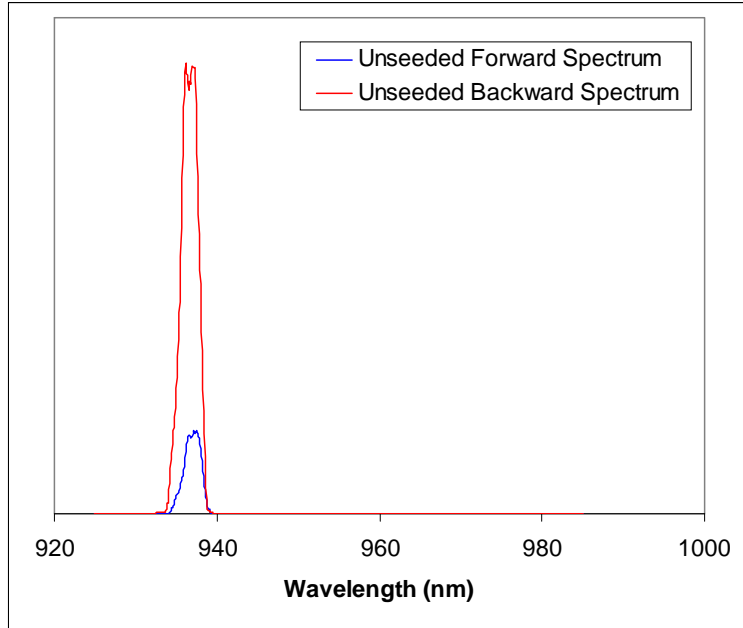


Figure 3.3: Spectrum results of both the forward (red) and backward (blue) directions for the single diode pumped, unseeded RFA based on the 1.8 km NuFern GRIN 100  $\mu\text{m}$  core fiber. The unseeded spectrum verifies there is no Stokes conversion of the pump, even at maximum pump power.

in the forward direction, and a very defined peak in the backward direction. In this case, both lasers were given over 30 minutes to stabilize. As a result, the peaks in both directions, and for both wavelengths, correspond favorably.

**3.3.2 Power Data.** Power data was also taken for both residual pump (figure 3.6), and backward Stokes powers (figure 3.7), for these three scenarios. Based on these results, it was shown that the fiber in question does allow for seed gain at the Stokes wavelength, but only for the seeded configurations. Since there was no Stokes generated in the unseeded configuration, the total backward power difference between the seeded configurations and the unseeded configuration was assumed to be the Stokes power gain. In the .5 watt seeded configuration, approximately 45 mW of Stokes power was converted from the pump, where as 55 mW of conversion resulted from the 1.3 W seeded arrangement. Based on the ratios of total output power at the seed wavelength to the input seed power, these values correspond to 22.6% and 23.6%

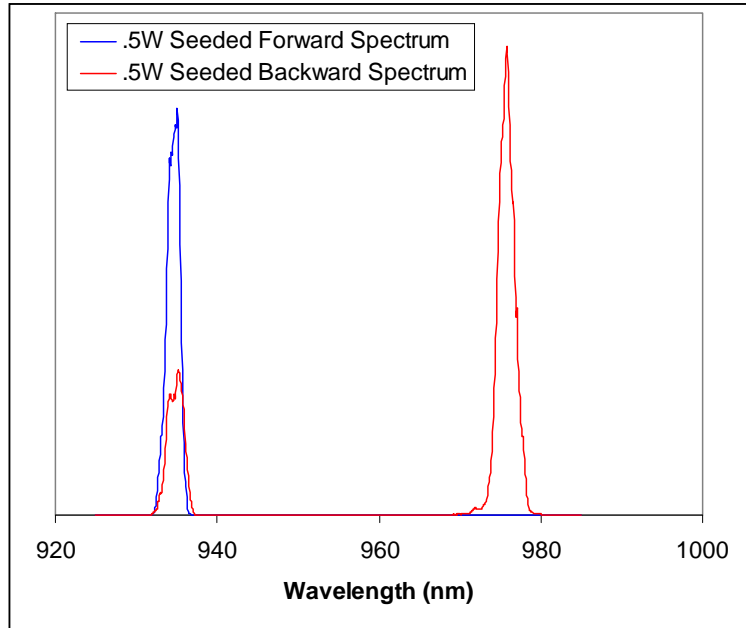


Figure 3.4: Spectrum data for the .5 W seeded configuration based on the 1.8 km NuFern GRIN 100  $\mu\text{m}$  core fiber. The spectrum shows the spectrum of the backward Stokes in blue and the residual pump in red. The slight shift in the pump wavelength peak between the two points can be attributed to a lack of warm-up time for the pump laser.

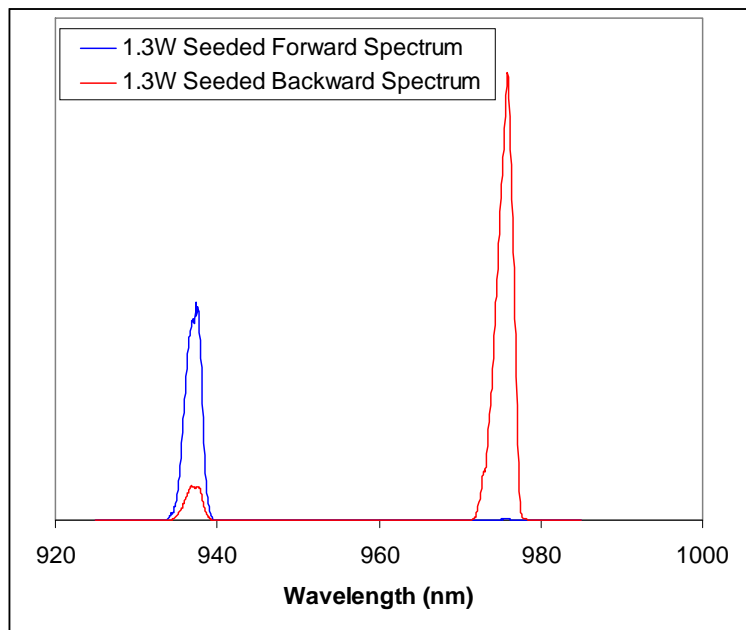


Figure 3.5: Spectrum for the 1.3 W seeded single diode pumped RFA configuration based on the 1.8 km NuFern GRIN 100  $\mu\text{m}$  core fiber.

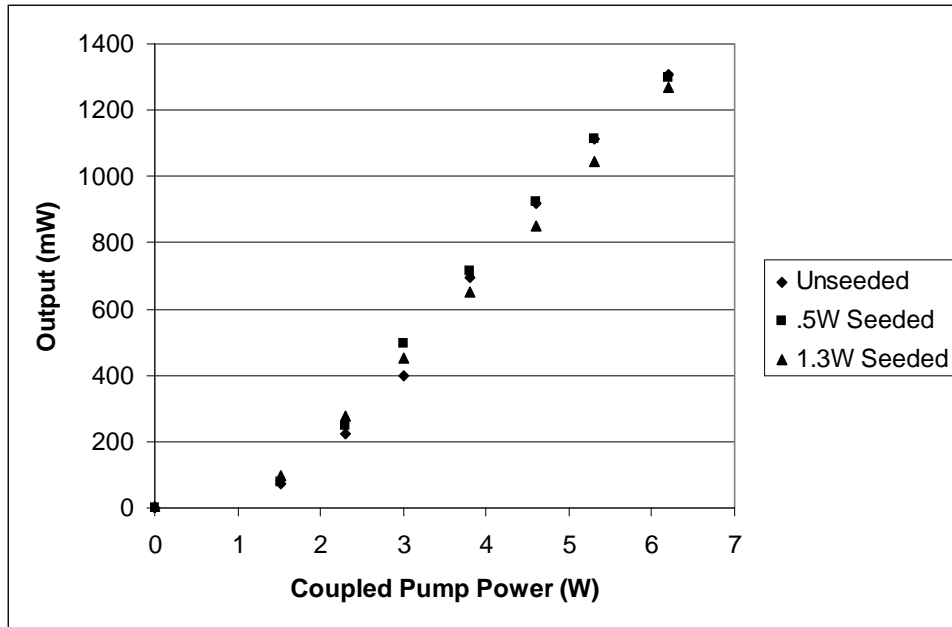


Figure 3.6: Single diode pumped residual pump power data for the unseeded, .5 W seeded , and 1.3 W seeded configurations.

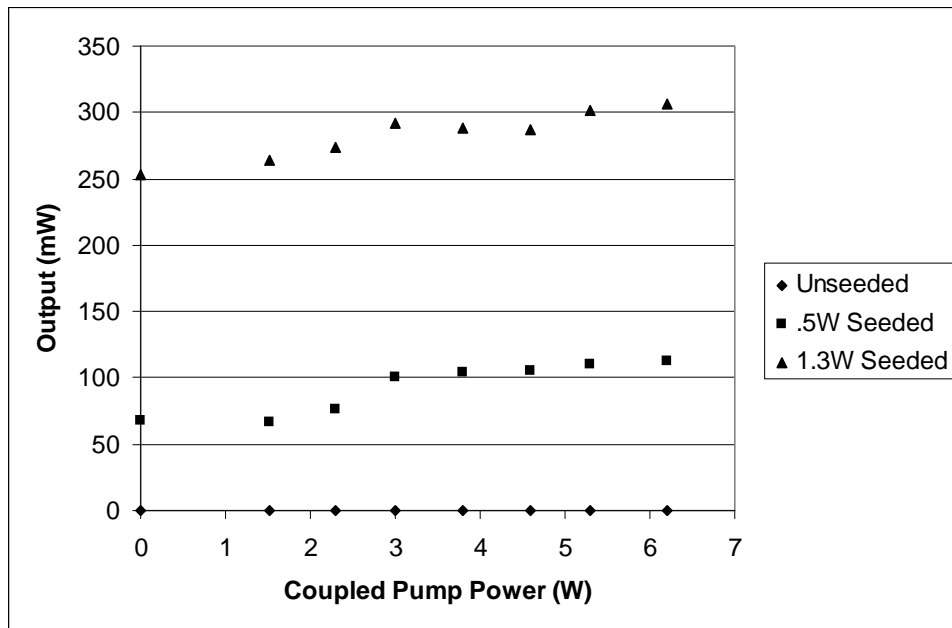


Figure 3.7: Single diode pumped backward Stokes power data for the unseeded, .5 W seeded, and 1.3 W seeded configurations.

of the input coupled seed power, respectively, but represent an average conversion efficiency of the pump of only .7% and .9%, based on the ratio of the total amount of Stokes power gain to the total amount of coupled pump power. The maximum conversion efficiency achieved for both seeded tests were 3.4% for the .5 W seeded, and 2.6% for the 1.3 W of seed, both at 3 W of coupled pump power.

### ***3.4 Summary***

This experiment verified that Raman gain is possible using poor beam quality, diode lasers as both pump and seed lasers in this fiber. This lays the foundation for using the multiple-beam combiner to couple four LIMO diode lasers at once into the gain fiber. Based on these results, more pump power should allow for better Stokes conversion within the fiber, and higher output power as well.

## IV. Multi Diode Pumped $100\ \mu\text{m}$ GRIN 1.8 km RFA

### 4.1 *Experimental Setup*

Once gain was shown to be possible, the next step was to couple more pump power into the gain fiber, in hopes of achieving amplification. Because the LIMO diodes used for the pumps are only rated at 25 W maximum output, it was necessary to use a squid-like fiber beam combiner to couple the beams from multiple pump diodes into one, more powerful beam. The beam combiner used was a seven channel OFS brand beam combiner, with an input core size of  $100\ \mu\text{m}$  and NA of .22. This matches the output fiber from the pump lasers very well, so free space coupling should have been very efficient. This, however, was not the case, as maximum coupling efficiency achieved for any channel was only 55%. Because the input channels of the squid were only rated at 15 watts per channel, high pump powers resulted in fiber facet damage of the squid during free space coupling. Different focusing microscope objectives were tested to maximize efficiency, while limiting fiber damage at higher powers. The use of 16x focusing objectives was found to be the best for this configuration, but limited the coupled power to a maximum of 12 watts per channel, with an average of only 9 watts per channel. A schematic of the setup, which mimics that of experiment 1, is shown in figure 4.1.

The output fiber of the squid presented another problem in this experiment. Whereas the gain fiber was  $100\ \mu\text{m}$  core and .29 NA, the output fiber of the fiber beam combiner had an NA of .45 and core size  $125\ \mu\text{m}$ . Based on the etendue value described above, a rough estimate of the maximum coupling efficiency that can be achieved between these two fibers is approximately 27%. With an average of only 9 watts per channel coupled into the squid, corresponding to 36 watts of total output for the 4 pump diodes used, only 10.4 watts of pump power was measured to be coupled into the gain fiber, or 28% of the output squid power. While still greater than the power of a single diode, the use of four diode lasers only achieved a 70% increase in coupled power into the gain fiber.

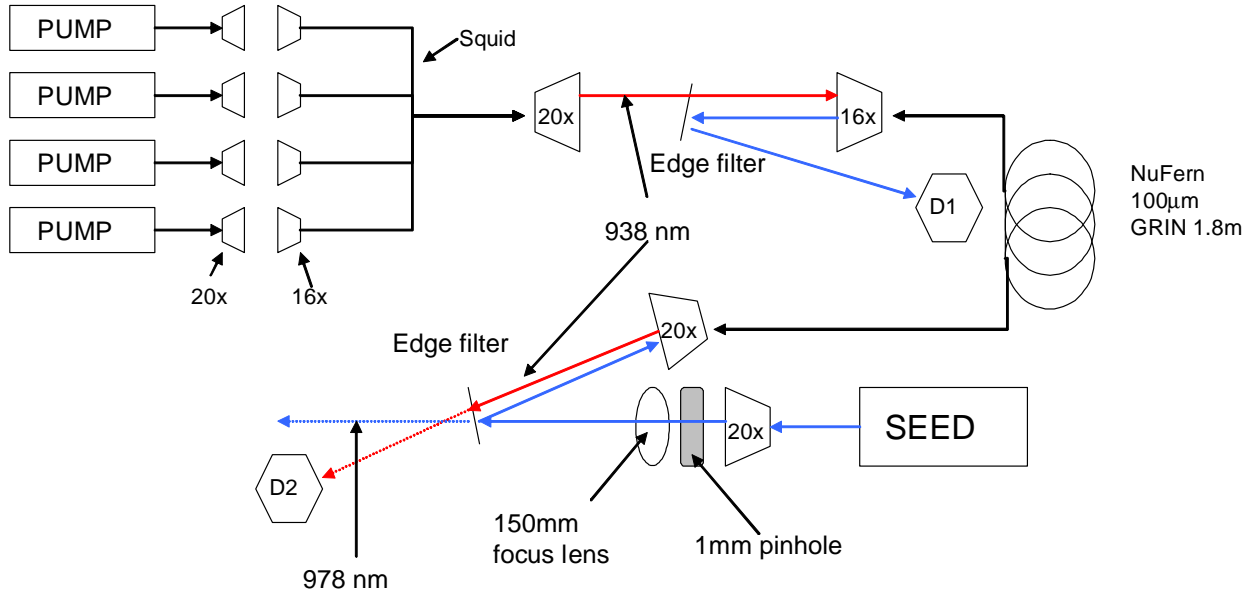


Figure 4.1: Schematic of experiment 2. All 4 pump diodes are collimated using 20x microscope objectives, and subsequently focus into the squid with 16x objectives. Again, D1 and D2 are diagnostic points.

## 4.2 Experiment 2 Results

**4.2.1 Spectrum Data.** For this experiment, spectrum measurements were taken for both an unseeded configuration, as well as a 3.5 W of coupled seed arrangement. Both the forward and backward spectrums were taken at maximum pump power. The spectrum data for the unseeded configuration can be seen in figure 4.2.

The spectrum of the unseeded setup again confirms that Raman threshold was not reached with the amount of pump power present in the fiber, as there is no Stokes beam generated. Another important factor to note is that all four diode pumps had to be calibrated so they would operate at the same wavelength throughout the range of currents. This was achieved by adjusting the operating temperature of each diode for a given current, until satisfactory overlapping of the peaks occurred. As evident from the spectrum in figure 4.2, the results were quite impressive, with only a small amount of shift between the peaks. With 3.5 W of seed power, the spectrum for both Stokes and residual pump were taken again. The results can be seen in figure 4.3.

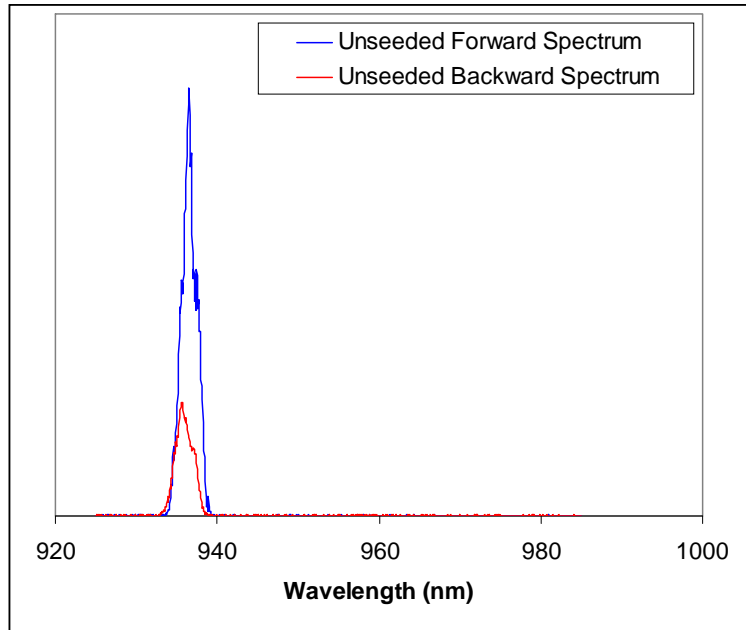


Figure 4.2: Spectrum for the unseeded multi-diode pumped RFA configuration based on the 1.8 km NuFern GRIN 100  $\mu\text{m}$  core fiber.

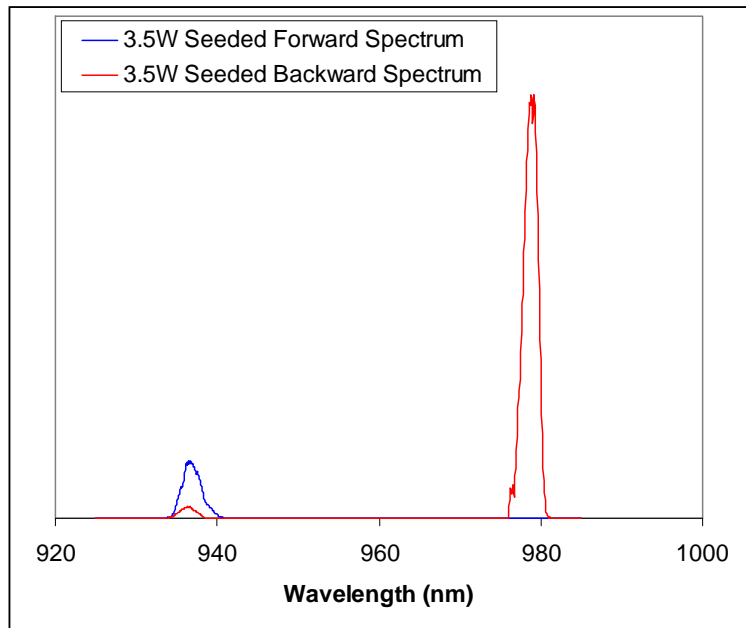


Figure 4.3: Spectrum for the 3.5 W seeded multi-diode pumped RFA configuration based on the 1.8 km NuFern GRIN 100  $\mu\text{m}$  core fiber.



The seeded spectrum shows a minimal amount of pump still present in the backward output. This is largely due to reflections of the pump light at fiber facets and optics, and also to the less than 100% transmission of the pump light at the edge filters.

*4.2.2 Power Data.* Again, power measurements were taken for both the seeded and unseeded arrangements. All backward measurements (figure 4.5) were taken at position D1, and all forward (figure 4.4) at position D2 on the schematic. The results of the power measurements show that gain is again present in the fiber, but

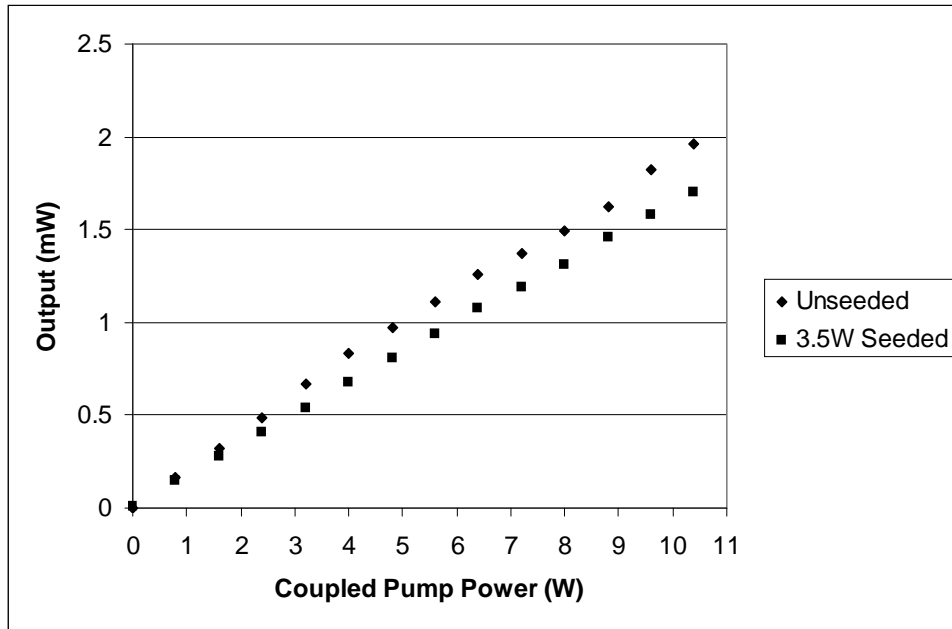


Figure 4.4: Multi-diode pumped residual pump power data for the unseeded and 3.5 W seeded configurations for the 100  $\mu\text{m}$  core GRIN fiber.

not amplification. As in experiment 1, there was no Stokes generated in the unseeded arrangement, but over 200mW of conversion was shown with 3.5 W of seed and 10.4 W of pump. This value corresponds to 33% of the coupled seed power, calculated as described above, which is a 10% gain over the single diode configuration. The average conversion efficiency for this test was approximately 2.2%, with a peak of over 6.2%, as seen in figure 4.6.

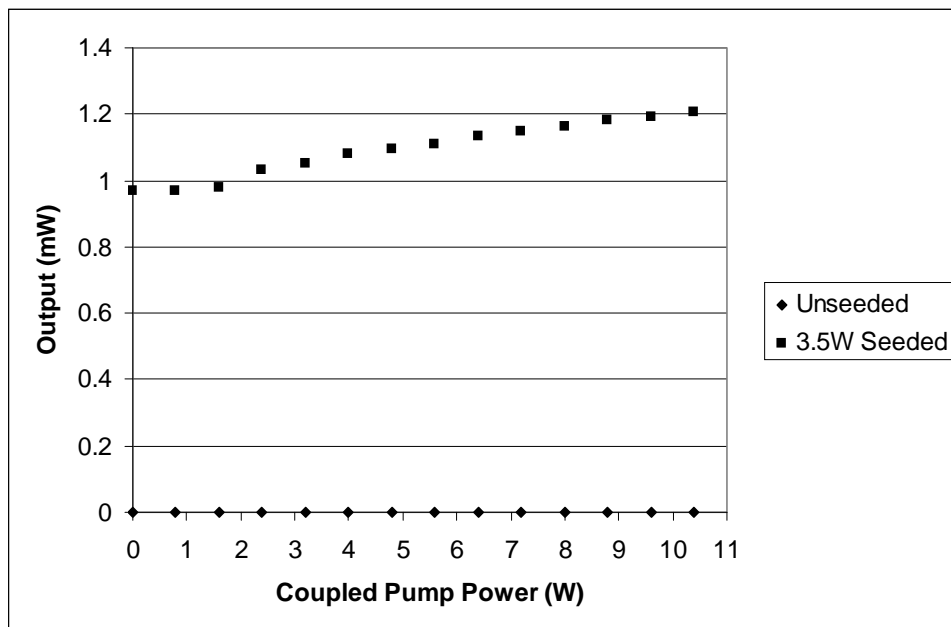


Figure 4.5: Multi-diode pumped backward Stokes power data for the unseeded and 3.5 W seeded configurations based on the 100  $\mu\text{m}$  core GRIN fiber.

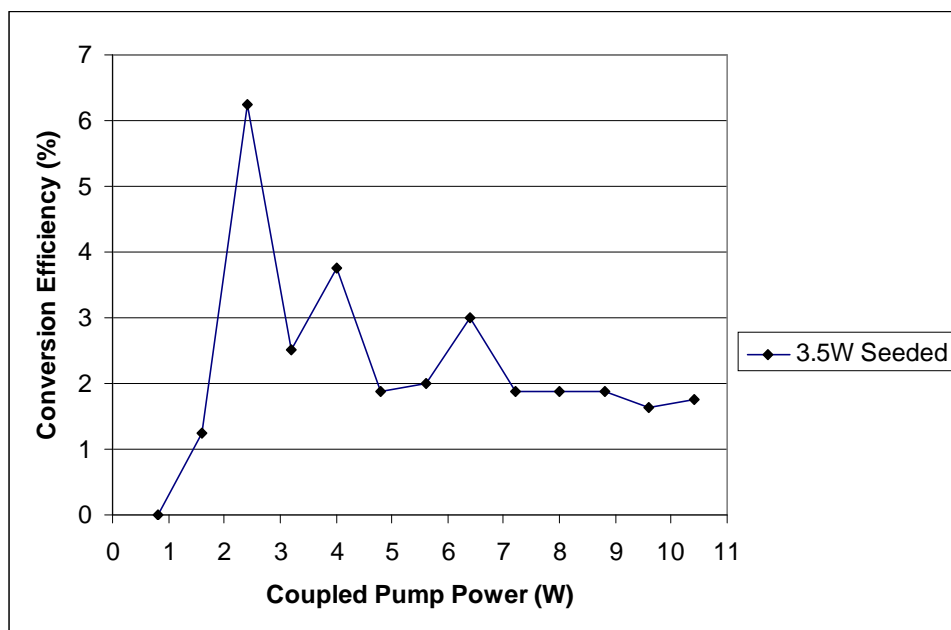


Figure 4.6: The Stokes conversion efficiency for Experiment 2. The average for this experiment is approximately 2.2%, with the peak being 6.25%.

		Unseeded		3.5W Seeded	
Coupled Pump Power	Error	Residual Pump	Stokes	Residual Pump	Stokes
(W)	(+/-W)	Error (+/-W)	Error (+/-W)	Error (+/-W)	Error (+/-W)
0	0	0.000	0	0.000	0
0.8	0.0007	0.001	0.007	0.000	0.0014
1.6	0.0014	0.001	0.014	0.000	0.0028
2.4	0.0016	0.001	0.016	0.000	0.0032
3.2	0.0018	0.002	0.018	0.000	0.0036
4	0.0025	0.003	0.025	0.000	0.005
4.8	0.0031	0.003	0.031	0.000	0.0062
5.6	0.0034	0.003	0.034	0.001	0.0068
6.4	0.0036	0.004	0.036	0.001	0.0072
7.2	0.0044	0.003	0.044	0.001	0.0088
8	0.0049	0.003	0.049	0.001	0.0098
8.8	0.0051	0.003	0.051	0.001	0.0102
9.6	0.0057	0.003	0.057	0.001	0.0114
10.4	0.0061	0.004	0.061	0.001	0.0122

Figure 4.7: Measurement errors for the multi-diode pumped RFA based on the 100  $\mu\text{m}$  core, 1.8 km long GRIN fiber. Error includes power fluctuations in the laser and calibration of power meters.

### 4.3 Beam Quality

One of the inherent properties of Raman scattering in an unseeded configuration is its ability to produce a good quality Stokes beam. By measuring the  $M^2$  value of the pump, seed, and amplified seed beams, this property should still be apparent, even when using very poor quality diodes as both the pump and seed lasers. To measure these values, the Coherent ModeMaster camera described above was used. Figure 4.8 shows the placement of the camera used to record these measurements. Because space was limited on the optics table, mirrors were used to pick off the beams, so they could propagate straight into the ModeMaster. The beam qualities of both the pump and amplified seed were taken after propagation through the fiber, and with the pump at maximum power, while the unamplified seed was taken with no pump present. The results show an unamplified seed beam quality factor of  $49.23 \pm 0.5$ , and an  $M^2$  value of  $43.01 \pm 0.5$  for the pump. When the seed is amplified, the  $M^2$

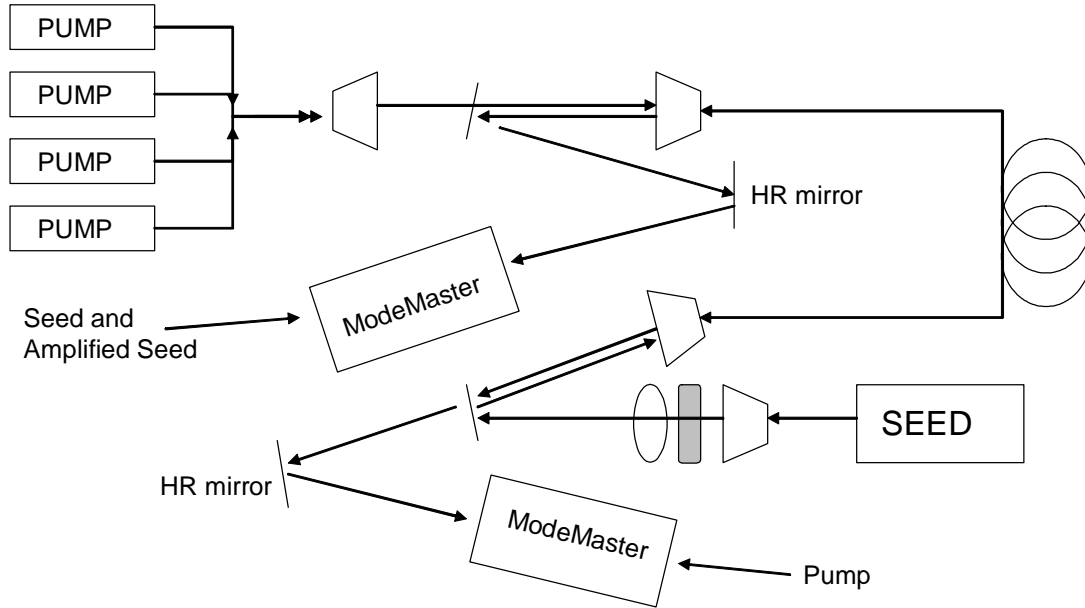


Figure 4.8: Schematic of the camera placement for taking  $M^2$  measurements.

factor was improved slightly, to  $47.05 \pm 0.5$ , showing that beam cleanup does still occur in multimode fibers, but is limited to the beam quality of the input seed.

#### 4.4 Summary

Based on measurements taken, a multi-diode pump system does allow for better gain and Stokes conversion when compared to a single diode pump, but is nowhere near achieving amplification. One of the key difficulties in conducting this experiment was free space coupling of the pump power into both the squid and the gain fiber. Because the etendue differences in the output fiber of the squid and the gain fiber severely limit the power coupled into the gain fiber, sufficient pump power needed to reach amplification was not achieved. The power measurements show that with greater coupled pump power, Stokes conversion is increased, along with gain at the seed wavelength. Using a different gain fiber, one with a better match to the output fiber of the squid, should allow for more coupled pump power, and ultimately greater Stokes conversion, if the effective core diameter remains relatively small. This is the basis for experiment 3, which utilizes a fiber comparable in parameters to the fiber

used in experiments 1 and 2, but with a  $200\mu\text{m}$  core instead. The larger core will allow for more light to be coupled into the fiber, but will also increase the power needed to achieve Raman threshold.

## V. Multi Diode Pumped 200 $\mu\text{m}$ core GRIN 2 km RFA

### 5.1 *Experimental Setup*

Based on the results of experiments 1 and 2, more coupled pump power into the fiber does allow for a higher overall seed gain. To achieve even higher gain, a fiber whose etendue that matches the output fiber of the squid should allow for better coupling efficiency, and possibly more gain, if the intensity within the larger fiber remains high. For this reason, a 2 km long, 200  $\mu\text{m}$  core fiber was used as the gain medium for this experiment. The trade-off to using a larger core fiber is increased threshold power, which is estimated to be around 130 watts for this fiber, assuming single mode operation. The experimentally determined attenuation for both the pump and seed wavelengths were 2.8 dB/km and 2.5 dB/km, respectively. These values correspond to a loss in the fiber of 70% of the pump light, and 65% of the seed power, which is very comparable to the 73% pump losses and 69% seed losses in the 100  $\mu\text{m}$  core fiber used previously. The NA for the 200  $\mu\text{m}$  core fiber was given by NuFern to be .275, which, according to conservation of etendue, will allow for almost 95% of the pump light to be coupled into the fiber, which corresponds to approximately 34 watts. The diagram for experiment 3 is similar to that of experiment 2, and can be seen in figure 5.1.

### 5.2 *Experiment 3 Results*

*5.2.1 Spectrum Data.* Spectrum measurements were again taken of both the forward and backward outputs, for both the seeded and unseeded configurations. As in the previous two experiments, these measurements were taken at maximum pump power, and from the two respective diagnostic points shown in the setup diagram. As expected, the unseeded spectrum shows no Stokes generation, evident by figure 5.2. The seeded spectrum, conducted with 3.5W of coupled seed power as in experiment 2, is shown in figure 5.3. As in experiment 2, a minimal amount of pump light is allowed to pass through the Stokes due to reflection at optics and transmission properties of the edge filters used.

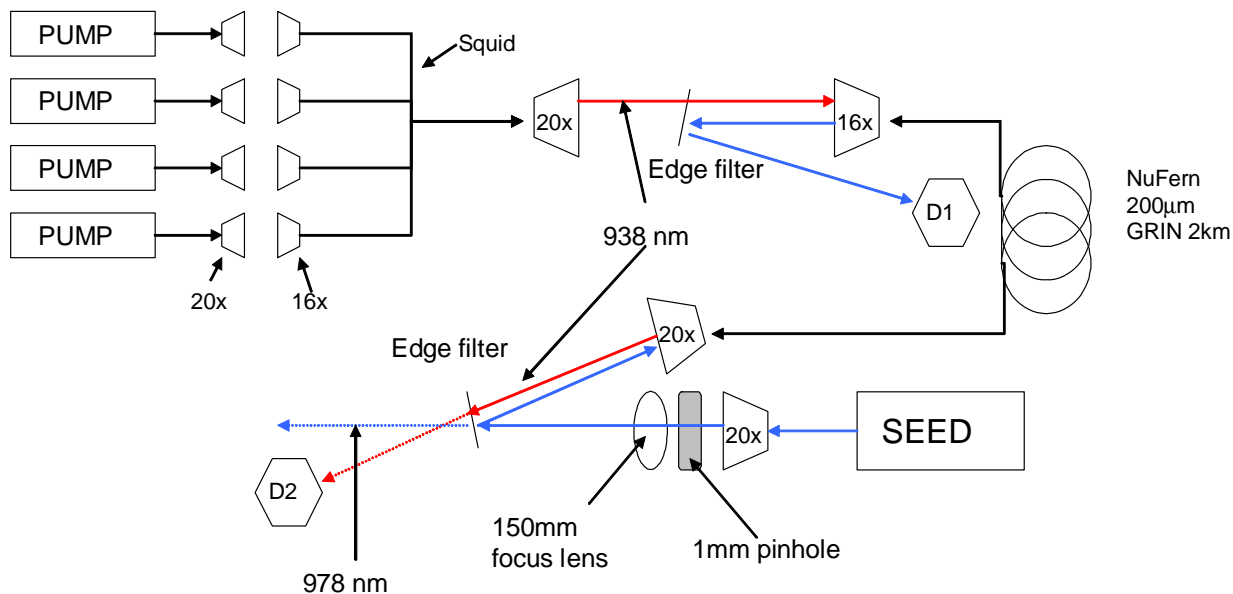


Figure 5.1: Schematic of experiment 3. Identical to that of experiment 2, but with a 2km NuFern 200  $\mu\text{m}$  core GRIN fiber as the gain medium. D1 and D2 are diagnostic points. Again, a 16x microscope objective was determined to be the most efficient at coupling the pump power into the gain fiber.

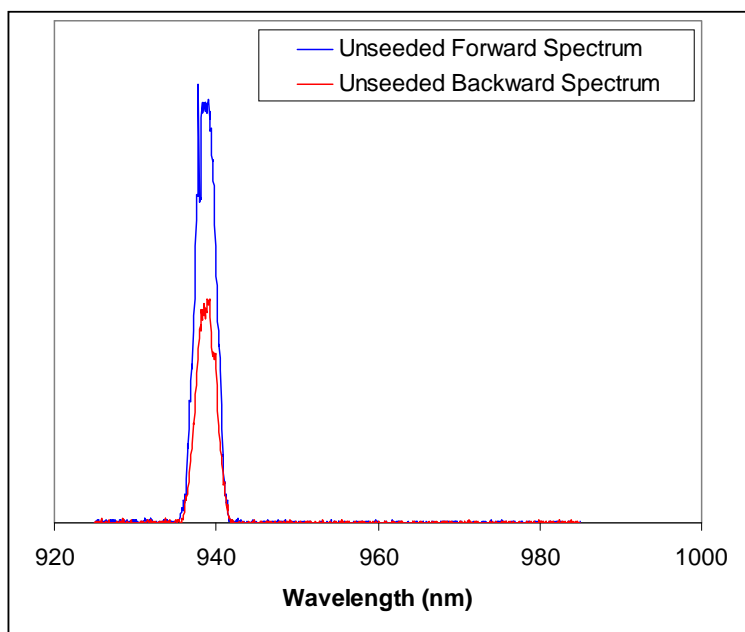


Figure 5.2: Spectrum for the unseeded multi-diode pumped RFA configuration based on the 2 km NuFern GRIN 200  $\mu\text{m}$  core fiber.

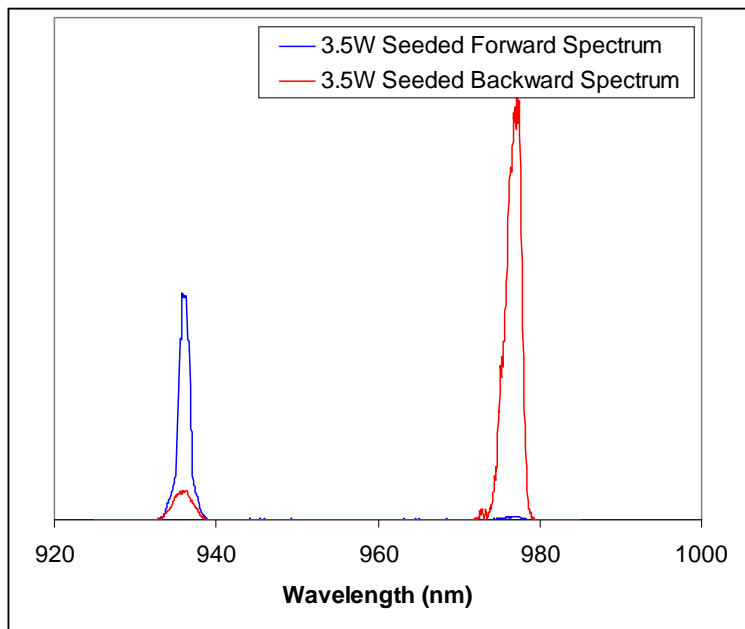


Figure 5.3: Spectrum for the 3.5 W seeded multi-diode pumped RFA configuration based on the 2 km NuFern GRIN 200  $\mu\text{m}$  core fiber.

**5.2.2 Power Data.** As in experiment 2, measurements were taken of power outputs at point D2 and D1 on the schematic, corresponding to the residual pump power and backward Stokes power, respectively. The results for the residual pump powers are shown in figure 5.4, and the backward Stokes power in figure 5.5. Because the Raman threshold for this fiber approximately twice that of the previous fiber, pump conversion occurred at higher powers, as evident by the data in figure 5.4. The two slopes begin to diverge around 3.25 watts for this fiber, whereas the 100  $\mu\text{m}$  core fiber showed pump conversion beginning at around 1.6 watts. The total maximum pump power absorbed was approximately 850 mW, or 6% of the total coupled pump power. The backward Stokes power again shows no unseeded Stokes generation, and a seeded gain of approximately 80mW, or about 2.5% of the total coupled seed power. This value corresponds to an overall seed output of only 18.5%, more than 10% lower than the previous experiment. The average conversion efficiency for this experiment, shown in figure 5.6, was only .6%, with a high of 1.3%.



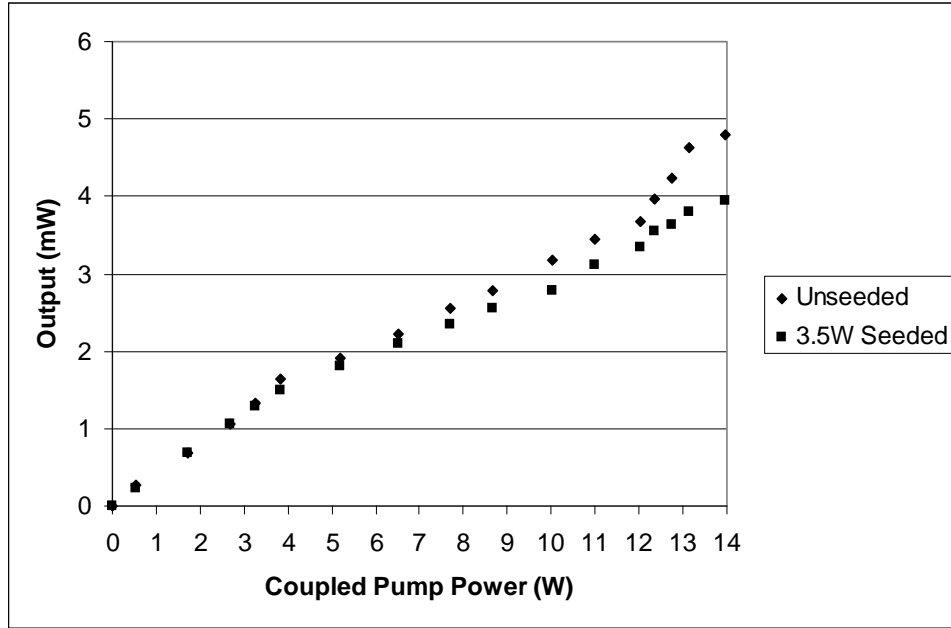


Figure 5.4: Multi-diode pumped residual pump power data for the unseeded and 3.5 W seeded configurations based on the 200  $\mu\text{m}$  core GRIN fiber. A decrease in the maximum residual pump power of approximately 800mW between the unseeded and seeded configuration is shown.

### 5.3 Beam Quality

$M^2$  measurements were taken according to the schematic shown in figure 4.8. The pump beam produced an  $M^2$  of  $56.63 \pm 0.5$ , and the seed an  $M^2$  of  $67.4 \pm 0.5$ . The amplified seed showed only slight improvement over the seed, with an  $M^2$  of  $66.4 \pm 0.5$ , further reinforcing the belief that the amplified seed quality is limited to the quality of the seed itself.

### 5.4 Summary

Although conservation of etendue suggested a maximum coupling efficiency of 95%, or 34 watts, only 14 watts was able to be coupled into the fiber, approximately 40%. This is 130% of the power coupled into the previous fiber, but the Raman threshold for this fiber is roughly 4 times that of the 100  $\mu\text{m}$ , as Raman threshold is proportional to the cross-sectional area of the fiber. This was apparent in the power measurements taken for the both Stokes and residual pump, as conversion of

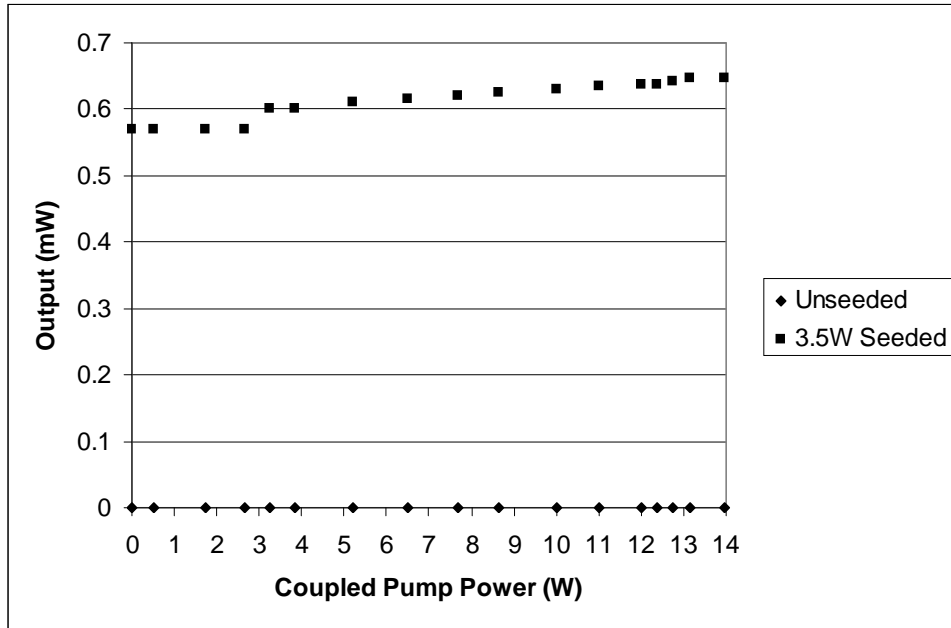


Figure 5.5: Multi-diode pumped backward Stokes power data for the unseeded and 3.5 W seeded configurations based on the 200  $\mu\text{m}$  core GRIN fiber. Based on spectrum results, no Stokes was generated in the unseeded experiment, but over 650mW is shown with a seed present, at maximum pump power of 14 watts.

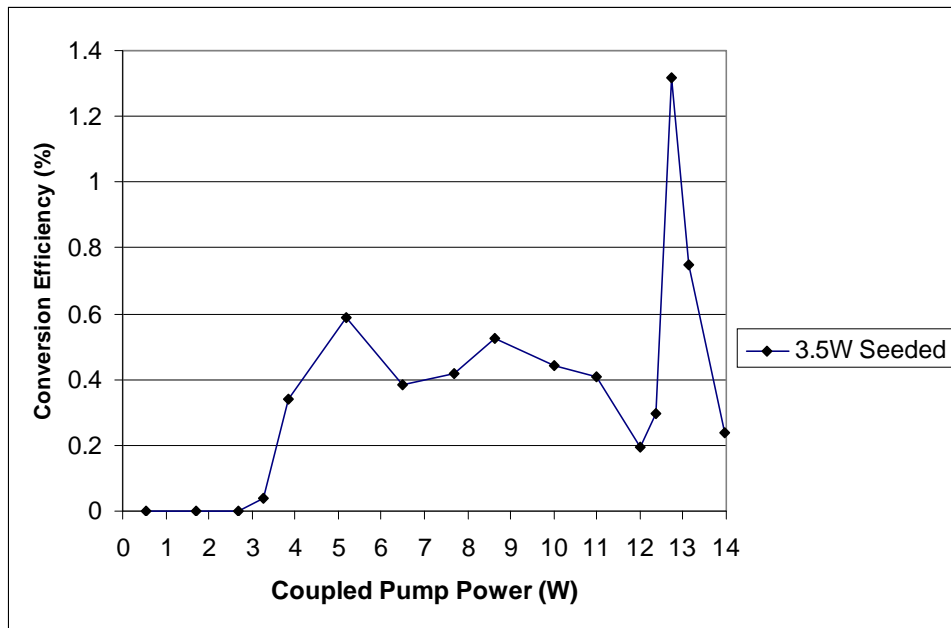


Figure 5.6: The Stokes conversion efficiency for Experiment 3. The average for this experiment is approximately 0.6%, with the peak being 1.3%.

Coupled Pump Power (W)	Error (+/-W)	Unseeded		3.5W Seeded	
		Residual Pump	Stokes	Residual Pump	Stokes
		Error (+/-W)	Error (+/-W)	Error (+/-W)	Error (+/-W)
0	0.000	0	0.000	0.000	0.000
0.53	0.001	0.008	0.001	0.012	0.000
1.72	0.002	0.007	0.003	0.011	0.001
2.67	0.003	0.004	0.005	0.006	0.002
3.25	0.004	0.005	0.006	0.008	0.002
3.84	0.005	0.008	0.008	0.012	0.003
5.2	0.006	0.005	0.011	0.008	0.004
6.5	0.007	0.006	0.012	0.009	0.005
7.7	0.008	0.006	0.014	0.009	0.006
8.65	0.010	0.01	0.016	0.015	0.007
10.01	0.011	0.008	0.019	0.012	0.007
10.99	0.012	0.006	0.020	0.009	0.008
12.02	0.012	0.009	0.021	0.014	0.008
12.36	0.013	0.006	0.021	0.009	0.008
12.74	0.014	0.007	0.023	0.011	0.009
13.14	0.015	0.008	0.024	0.012	0.010
13.98	0.015	0.01	0.025	0.015	0.010

Figure 5.7: Measurement errors for the multi-diode pumped RFA based on the 200  $\mu\text{m}$  core, 2 km long GRIN fiber. Error includes power fluctuations in the laser and calibration of power meters.

the pump power was shown to begin at approximately 3.6 W, almost twice that of the previous fiber. Amplification was not achieved, and an overall Stokes conversion efficiency was shown to be only 0.6%, well below that of experiment 2. The core size of the fiber used in this experiment pushes the Raman threshold beyond what can be achieved with this setup. An alternative to the large core size fiber, and the basis for the fiber experiment, is to use a DCF as the gain fiber. The high NA of the inner cladding should allow for sufficient pump light to be coupled in, while the smaller core size should keep the Raman threshold down to levels achievable for the pump source used.

## VI. Multi Diode Pumped 50/250 DCF 500m RFA

### 6.1 *Experimental Setup*

Based on the results of experiments 2 and 3, more coupled pump power into the fiber, along with a smaller core size, allows for better Stokes conversion. To achieve this, a fiber whose etendue that matches the output fiber of the squid, and whose core size is as small as possible, should allow for better coupling efficiency, and ultimately more gain. For this experiment, a 500m long, DCF with a  $50\ \mu\text{m}$  core and a  $250\ \mu\text{m}$  inner cladding was used as the gain fiber. The  $50\ \mu\text{m}$  core reduces the single mode Raman threshold to approximately  $32\text{W}$ , a value well within the limits of the pump source. The main concern here is that sufficient pump power will not be absorbed into the core, as the inner cladding has an NA of .46, but the core an NA of only .28. Attenuation of the fiber at pump and seed wavelength were determined experimentally to be  $12.1\text{dB/km}$  and  $9.5\text{dB/km}$ , respectively, which is comparable in power losses to the  $100\ \mu\text{m}$  core fiber used above, as the length of the DCF fiber is 25% of the  $100\ \mu\text{m}$  fiber, but with 4 times the attenuation per kilometer. Because a DCF allows for propagation of the beam in the inner cladding, the conservation of etendue between the squid and gain fiber was based on the parameters of the inner cladding. This value specifies a 100% possible coupling between these two fibers, but was experimentally determined to be approximately 70%, due mainly to losses at the optics and fiber facets.

The setup for experiment 4 is similar to that the earlier two, and is shown in figure 6.1. The spatial filter for the seed laser was left in place to maximize the beam quality coupled into the fiber. Because the DCF has a smaller core, a higher quality beam, one with lower order modes, should be more readily coupled into the core. The hope is that the poor beam quality of the pump will also be coupled into the core, where conversion to the Stokes wavelength is more likely than in the inner cladding, as the core supports fewer modes than the inner cladding, and the Raman threshold is therefore much lower.

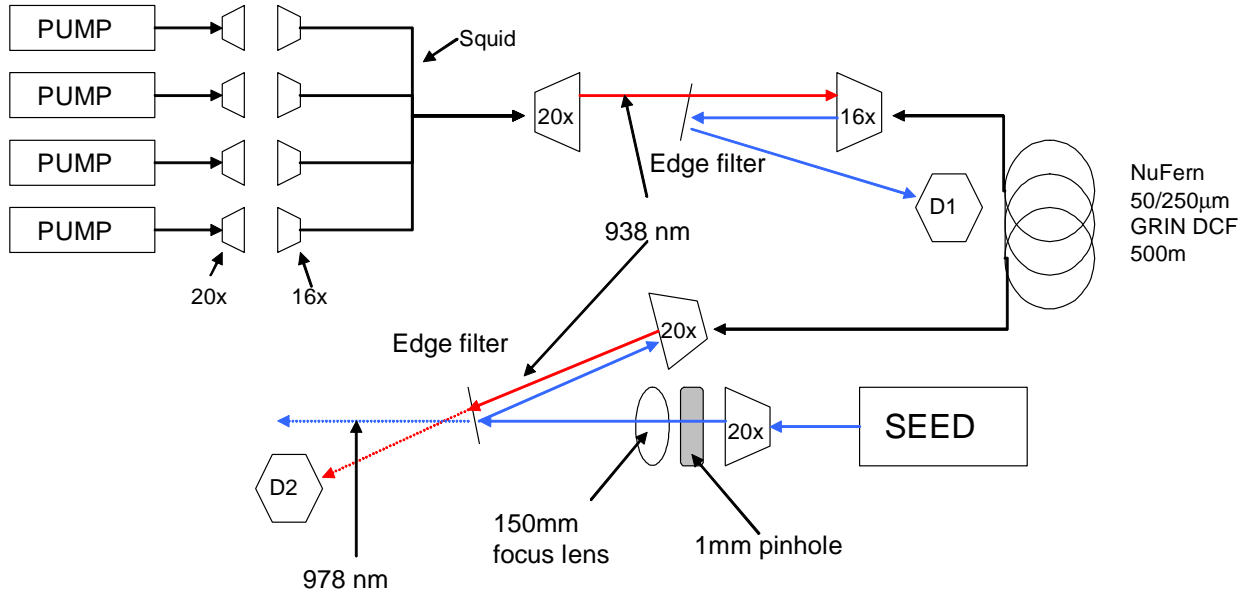


Figure 6.1: Schematic of experiment 4. Again, all 4 pump diodes are combined using the squid, with 36 watts of total output. The gain fiber used is a 50/250 NuFern GRIN core fiber at 500m in length. D1 and D2 are diagnostic points. The spatial filter for the seed was left in place to enhance the beam quality being coupled into the fiber.

## 6.2 Experiment 4 Results

**6.2.1 Spectrum Data.** As in the two previous experiments, spectrum data was taken for both seeded and unseeded configurations. Because the fiber allowed for better coupling of both the pump beam and seed beam, 4.2 watts of seed power was able to be coupled into the fiber, which corresponds to approximately 75% of the incident power. The unseeded spectrum, for both the forward and backward directions, can be seen in figure 6.2. As in previous experiments, Raman threshold was not achieved in the absence of a seed, as there was again no Stokes generation present in the spectrum. The seeded configuration, shown in figure 6.3, verifies the seed wavelength is positioned favorably for the Stokes shift, with a small amount of pump power still evident in the backward direction.

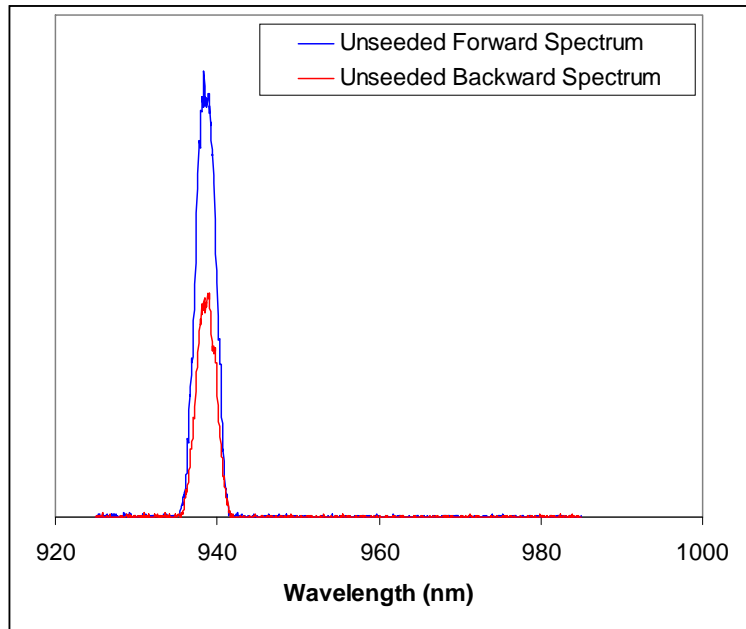


Figure 6.2: Spectrum for the unseeded multi-diode pumped RFA configuration based on the 500m NuFern GRIN 50/250  $\mu\text{m}$  DCF fiber.

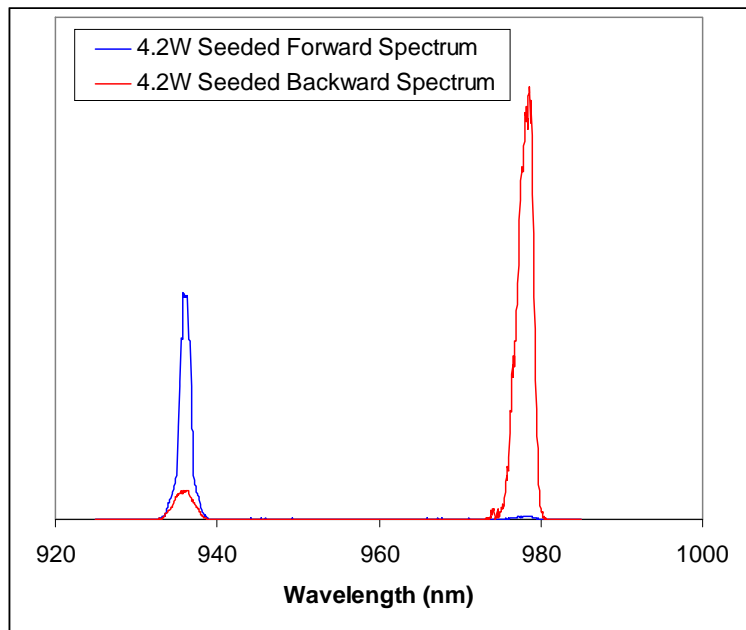


Figure 6.3: Spectrum for the 4.2 W seeded multi-diode pumped RFA configuration based on the 500m NuFern GRIN 50/250  $\mu\text{m}$  DCF fiber.

**6.2.2 Power Data.** Power data was again taken for both residual pump and backward Stokes power, at position D2 and D1 on the schematic, respectively. The residual pump power, figure 6.4, shows an 800mW decrease in the power between the unseeded and seeded configurations, at over 25 watts of coupled pump power. This value corresponds to approximately 3% of the total coupled pump power, or over 13% of the unseeded maximum residual pump power. Based on previous experiments, we should have seen a Stokes power increase of over a half a watt, but this was not the case, as evident by figure 6.5, the power data for the backward Stokes. Instead, only 103 mW of gain in the Stokes was shown, which relates to an average conversion efficiency of less than 0.5%. The maximum conversion efficiency for this experiment was calculated at 0.8%, shown in figure 6.6.

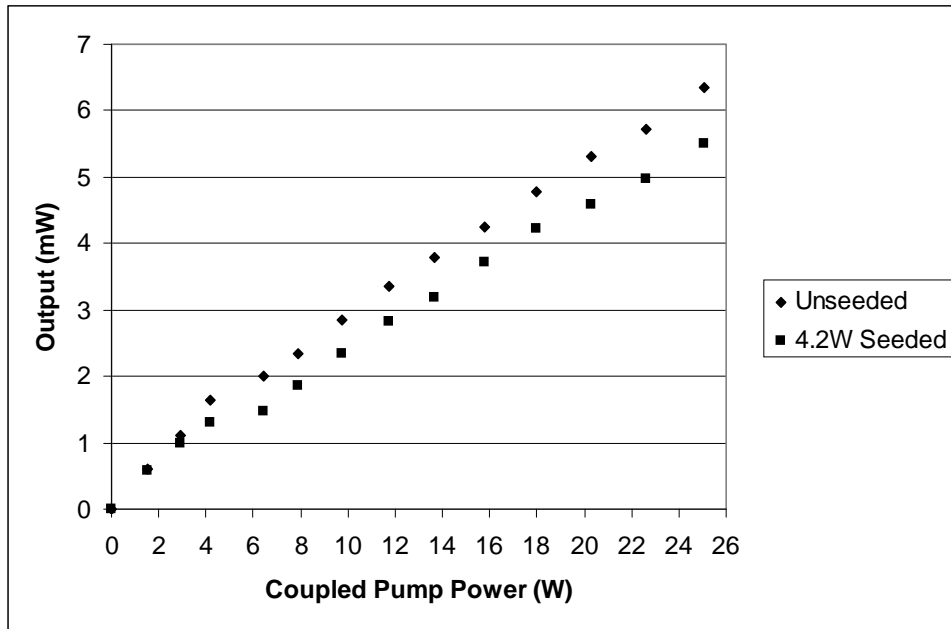


Figure 6.4: Multi-diode pumped residual pump power data for the unseeded and 4.2 W seeded configurations based on the 50/250  $\mu\text{m}$  core DCF GRIN fiber. A decrease in the maximum residual pump power of approximately 800mW between the unseeded and seeded configuration is shown.

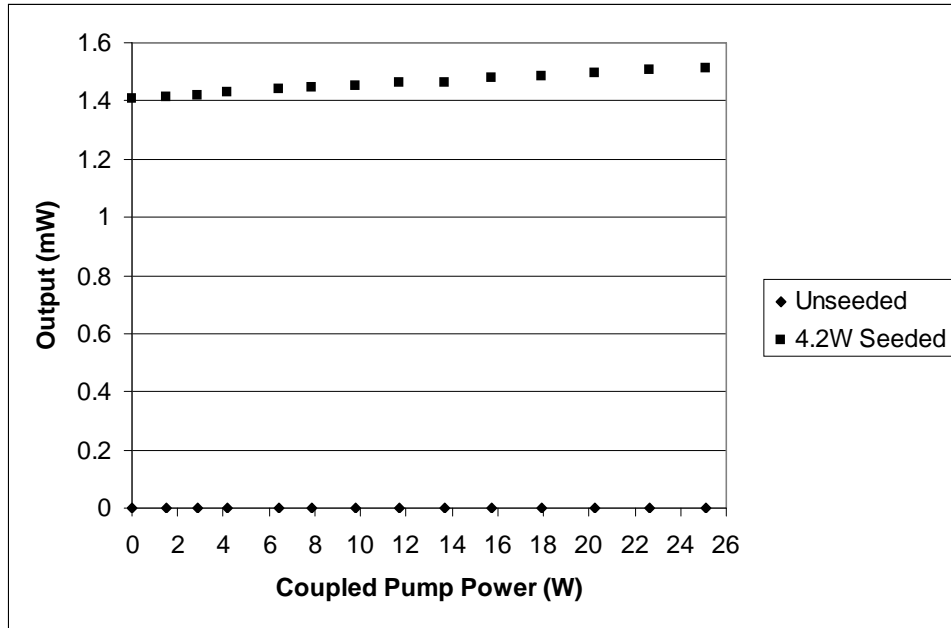


Figure 6.5: Multi-diode pumped backward Stokes power data for the unseeded and 4.2 W seeded configurations based on the 50/250  $\mu\text{m}$  core DCF GRIN fiber. Based on spectrum results, no Stokes was generated in the unseeded experiment, but over 1.5 watts is shown with a seed present, at maximum pump power of 25.1 watts.

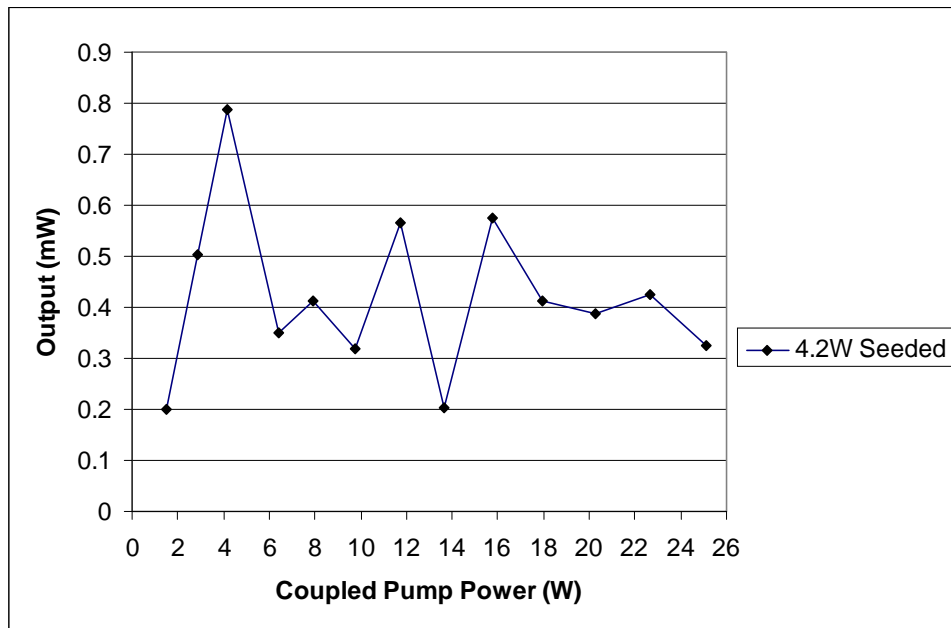


Figure 6.6: The Stokes conversion efficiency for Experiment 4. The average for this experiment is approximately 0.4%, with the peak being 0.8%.



Coupled Pump Power (W)	Error (+/-W)	Unseeded		4.2W Seeded	
		Residual Pump Error (+/-W)	Stokes Error (+/-W)	Residual Pump (+/-W)	Stokes (+/-W)
		0	0.000	0	0
1.5	0.003	0.001	0.005	0.002	0.001
2.89	0.005	0.002	0.008	0.003	0.0016
4.16	0.005	0.003	0.009	0.005	0.0018
6.44	0.006	0.005	0.01	0.008	0.002
7.89	0.009	0.006	0.015	0.009	0.003
9.77	0.011	0.003	0.018	0.005	0.0036
11.71	0.012	0.005	0.02	0.008	0.004
13.68	0.013	0.007	0.021	0.011	0.0042
15.77	0.014	0.007	0.024	0.011	0.0048
17.95	0.016	0.008	0.027	0.012	0.0054
20.27	0.017	0.006	0.028	0.009	0.0056
22.63	0.019	0.009	0.032	0.014	0.0064
25.1	0.020	0.01	0.034	0.015	0.0068

Figure 6.7: Measurement errors for the multi-diode pumped RFA based on the 50/250  $\mu\text{m}$  core, .5 km long GRIN DCF fiber. Error includes power fluctuations in the laser and calibration of power meters.

### 6.3 Beam Quality

Beam quality measurements of the pump, seed, and amplified seed show no apparent beam cleanup. The  $M^2$  of the pump was determined to be  $83.07 \pm .5$ , while the seed produced an  $M^2$  of only  $37.37 \pm .5$ . The amplified seed was actually slightly higher than the seed itself, having an  $M^2$  of  $37.88 \pm .5$ .

### 6.4 Summary

The results of this experiment were quite disappointing. Even with a 250% increase in the coupled pump power over the 100  $\mu\text{m}$  core used in the previous experiment, less than 50% of the total seed gain was shown. Because the NA of the core was only .28, compared to .47 of the output squid fiber, a majority of the pump power may have been confined to the inner cladding of the fiber, preventing the sufficient overlap between the pump and the seed needed for conversion, as the seed was able to propagate mainly in the core. The beam quality measurements show a pump  $M^2$

more than twice that of the seed, further reinforcing this hypothesis. The conversion efficiency was also low for this fiber, an average of only .4%, proving further that the pump and seed beams were not able to "interact" within the fiber.

## VII. Conclusions and Recommendations

### 7.1 *Results of this work*

The direct pumping of a Raman fiber amplifier (RFA) was attempted using an array of four 25W, fiber pigtailed diodes at 936nm, combined via a 7 channel fiber beam combiner. The initial attempt was conducted using a 1.8 km, 100  $\mu\text{m}$  core, GRIN fiber with an NA of .29 and attenuation 3.6 dB/km at 936nm. While amplification was not achieved, over 200mW of conversion was shown, with 10.4W of pump power and 3.5W of seed. This corresponds to an average conversion efficiency of 2.2%, and approximately 33% of the coupled seed power. One of the main deficiencies identified in this experiment was the amount of pump power able to be coupled into the gain fiber, due to the high NA of the output fiber of the squid. Because of this, the subsequent effort utilized a 2km long, 200  $\mu\text{m}$  core, GRIN fiber, with NA of .27 and attenuation of 2.8dB/km at pump wavelength. Again, amplification was not achieved, but a gain of 80mW was present, with 3.5W of seed power and 14W of pump. This corresponds to an average conversion efficiency of .6% and only 2.5% of the coupled seed power. The lack of amplification was more than likely a result of the high Raman threshold associated with this large core fiber. The final experiment attempted to solve both the problems of coupling efficiency and high Raman threshold by utilizing a 50/250 dual-clad fiber, with NAs of .28 and .46 for the core and inner cladding, respectively. Again, amplification was not realized, as only 100mW of gain was present, with 25W of pump and 4.2W of coupled seed power, corresponding to 36% of the coupled seed, and an average conversion efficiency of only .4%. The main problem identified with this experiment was the lack of mode overlap within the core of the fiber. Because the pump beam had such poor quality and high NA, sufficient power was not absorbed into the core, whereas a majority of the seed beam was. Although amplification was not achieved for any of the three fibers, gain was shown possible in all, showing that directly pumping an RFA with a diode source is possible.

## 7.2 *Suggestions for Future Work*

Throughout this experiment, there were many thoughts and ideas on how achieving a direct-diode pumped RFA could be made possible. The main problem with all three experiment was the lack of sufficient pump power able to be coupled into the core. This could be remedied with the use of a fiber beam combiner whose output NA is smaller, along with its core size, allowing for a smaller core gain fiber, and ultimately lower Raman threshold. This would require smaller fiber pigtailed for the pump diodes, which will be possible in the future, as the company who makes these diodes, LIMO, is offering a diode with a  $50\ \mu\text{m}$  core fiber output in the near future. This would also allow for a smaller core gain fiber, and, if the diodes are of sufficient power, may only need a single diode to achieve threshold.

Beam cleanup was also shown to be very limited with each of the three fibers, and was a result of the poor quality of the seed beam, as well as the backward pumping geometry of the amplifier, as shown by J. Morgan (9). A solution to this would be to utilize a higher quality seed beam, and/or pump the configuration in the forward geometry. The forward pumping of the seed would also lower the pump power needed to reach threshold, but may be effected by the cascading phenomenon due to FWM. The higher quality seed beam may allow for better overlap with the pump beam within the fiber.

## Appendix A. Calculating Raman Threshold

```

(*core radius*)
a := 50 * 10-6 (*m*)
(*fiber length*)
L := 1.8 * 103 (*m*)
(*attenuation at λ0 in dB/length*)
αdB := 3.2 * 10-3 (*dB/m*)
(*fiber numerical aperture*)
NA := .29
(*propagating wavelength*)
λ0 := 938 * 10-9 (*m*)
(*Raman gain coefficient for fused silica*)
gR := 1 * 10-13 (*m/W*)

(*attenuation in loss/length*)
αp =  $\frac{\alpha_{dB}}{4.353}$ 
0.000735125

(* V parameter*)
V = 2 π  $\frac{a}{\lambda_0}$  NA
97.1281

(*mode width parameter*)
w = a  $\left( \sqrt{\frac{2}{V} + \frac{.23}{V^{3/2}} + \frac{18.01}{V^6}} \right)$  (*m*)
7.18686 × 10-6

(*effective core area*)
Aeff = π w2 (*m2*)
1.62266 × 10-10

(*effective length of fiber due to losses*)
Leff =  $\frac{(1 - \text{Exp}[-\alpha_p L])}{\alpha_p}$ 
998.095

(*Raman threshold for backward Stokes generation, assuming GRIN core, random polarization of beam*)
Pth[Area_] := 2 *  $\frac{(20 \text{ Area})}{g_R L_{eff}}$  (*W*)

Pth[Aeff] (*this is the lower bound threshold power for this fiber, assuming only single mode operation... best case*)
65.0303

Pth[π a2] (*this is the upperbound threshold power for this fiber, assuming mode area is entire core area... worst case*)
3147.59

```

## Bibliography

1. Agrawal, Govind P. *Nonlinear Fiber Optics*. New York: Academic Press, 2001.
2. Chiang, K.S., "*Stimulated Raman Scattering in a Multimode Optical Fiber*," *Optics Letters*, Vol. 17, 352 (1992).
3. Baek, S.H. and Roh, Won B., "*Single-mode Raman fiber laser based on a multimode fiber*," *Optics Letters*, Vol 29, 153 (1994).
4. Flusche, B.M. et al., "*Multi-port beam combination and cleanup in a large multimode fiber using stimulated Raman scattering*," *Optics Letters*, Vol. 14, No. 24, (2006).
5. Terry, N.B. et al, "*Forward and backward seeded continuous-wave Raman fiber amplifiers based on multimode fibers*," 2006.
6. Federation of American Scientists website, <http://www.fas.org/spp/starwars/program/abl.htm>, Dec 2005.
7. Yariv, Ammon and Pochi Yeh, *Optical Waves in Crystals*. Hoboken: Wiley-Interscience, 2003.
8. Yablon, A.D., *Optical Fiber Fusion Splicing*, New York: Springer, 2005.
9. Morgan, J.D., "*Backward Amplification and Beam Cleanup of a Raman Fiber Laser Oscillator using a Multit-mode Graded Index Fiber Amplifier*," AFIT, 2006.
10. "*Encyclopedia of Laser Physics and Technology*," RP-Photonics, 2005
11. E.P. Ippen, "*Low-Power Quasi-CW Raman Oscillator*," *Appl Physics Letters*, 16, 303-305, 1970
12. "*Raman Spectroscopy, and overview*," Kaiser Optical Systems, Ann Arbor Michigan, 2001

**REPORT DOCUMENTATION PAGE**

*Form Approved  
OMB No. 074-0188*

The public reporting burden for this collection of information is estimated to average 1 hour per response, including the time for reviewing instructions, searching existing data sources, gathering and maintaining the data needed, and completing and reviewing the collection of information. Send comments regarding this burden estimate or any other aspect of the collection of information, including suggestions for reducing this burden to Department of Defense, Washington Headquarters Services, Directorate for Information Operations and Reports (0704-0188), 1215 Jefferson Davis Highway, Suite 1204, Arlington, VA 22202-4302. Respondents should be aware that notwithstanding any other provision of law, no person shall be subject to a penalty for failing to comply with a collection of information if it does not display a currently valid OMB control number.

**PLEASE DO NOT RETURN YOUR FORM TO THE ABOVE ADDRESS.**

<b>1. REPORT DATE (DD-MM-YYYY)</b> 22-03-2007		<b>2. REPORT TYPE</b> Master's Thesis		<b>3. DATES COVERED (From - To)</b> May 2005 - March 2007	
<b>4. TITLE AND SUBTITLE</b>  Direct Diode Pumped Raman Fiber Amplifier Based on a Multimode Graded Index Fiber				<b>5a. CONTRACT NUMBER</b>	
				<b>5b. GRANT NUMBER</b>	
				<b>5c. PROGRAM ELEMENT NUMBER</b>	
<b>6. AUTHOR(S)</b>  Baird, Charles J., Captain, USAF				<b>5d. PROJECT NUMBER</b>	
				<b>5e. TASK NUMBER</b>	
				<b>5f. WORK UNIT NUMBER</b>	
<b>7. PERFORMING ORGANIZATION NAMES(S) AND ADDRESS(S)</b> Air Force Institute of Technology Graduate School of Engineering and Management (AFIT/EN) 2950 Hobson Way WPAFB OH 45433-7765				<b>8. PERFORMING ORGANIZATION REPORT NUMBER</b>  AFIT/GAP/ENP/07-01	
<b>9. SPONSORING/MONITORING AGENCY NAME(S) AND ADDRESS(ES)</b>				<b>10. SPONSOR/MONITOR'S ACRONYM(S)</b>	
				<b>11. SPONSOR/MONITOR'S REPORT NUMBER(S)</b>	
<b>12. DISTRIBUTION/AVAILABILITY STATEMENT</b> APPROVED FOR PUBLIC RELEASE; DISTRIBUTION UNLIMITED.					
<b>13. SUPPLEMENTARY NOTES</b>					
<b>14. ABSTRACT</b> The direct pumping of a Raman fiber amplifier (RFA) was attempted using an array of four 25W, fiber pigtailed diodes at 936nm, combined via a 7 channel fiber beam combiner. The initial attempt was conducted using a 1.8 km, 100µm core, GRIN fiber with an NA of .29 and attenuation 3.6 dB/km at 936nm. While amplification was not achieved, over 200mW of conversion was shown, with 10.4W of pump power and 3.5W of seed. This corresponds to an average conversion efficiency of 2.2%. The subsequent effort utilized a 2km long, 200µm core, GRIN fiber, with NA of .27 and attenuation of 2.8dB/km at pump wavelength. Again, amplification was not achieved, but a gain of 80mW was present, with 3.5W of seed power and 14W of pump. This corresponds to an average conversion efficiency of 0.6% and only 2.5% of the coupled seed power. The final experiment attempted to solve the problem of coupling efficiency and high Raman threshold by utilizing a 50/250 dual-clad fiber, with NAs of .28 and .46 for the core and inner cladding, respectively. Again, amplification was not realized, as only 100mW of gain was present, with 25W of pump and 4.2W of coupled seed power, corresponding to 36% of the coupled seed, and an average conversion efficiency of only 0.4%. Although amplification was not achieved for any of the three fibers, gain was shown possible in all, showing that directly pumping an RFA with a diode source is possible.					
<b>15. SUBJECT TERMS</b> SRS, Raman Scattering, Raman Fiber Laser, Raman Fiber Amplifier, Backward Amplification					
<b>16. SECURITY CLASSIFICATION OF:</b>			<b>17. LIMITATION OF ABSTRACT</b>  UU	<b>18. NUMBER OF PAGES</b>  61	<b>19a. NAME OF RESPONSIBLE PERSON</b> Thomas Alley, LtCol, USAF
<b>REPORT</b> U	<b>ABSTRACT</b> U	<b>c. THIS PAGE</b> U			<b>19b. TELEPHONE NUMBER (Include area code)</b> (937) 255-6565, ext 4649; (Thomas.Alley@afit.edu)